

THESIS FOR THE DEGREE OF DOCTOR OF PHILOSOPHY

Lean NO_x reduction with methanol over supported silver catalysts

MARIKA MÄNNIKÖ

Department of Chemistry and Chemical Engineering
CHALMERS UNIVERSITY OF TECHNOLOGY
Gothenburg, Sweden 2015

Lean NO_x reduction with methanol over supported silver catalysts

MARIKA MÄNNIKKÖ

ISBN 978-91-7597-200-8

© MARIKA MÄNNIKKÖ, 2015.

Doktorsavhandlingar vid Chalmers tekniska högskola

Ny serie nr. 3881

ISSN 0346-718X

Department of Chemistry and Chemical Engineering

Chalmers University of Technology

SE-412 96 Gothenburg

Sweden

Telephone + 46 (0)31-772 1000

Cover: UV-vis spectra and NO_x reduction vs. temperature for four silver/alumina samples prepared by different methods. The illustration is based on figures included in section 5.2.

Chalmers Reproservice

Gothenburg, Sweden 2015

Lean NO_x reduction with methanol over supported silver catalysts

MARIKA MÄNNIKKÖ

Department of Chemistry and Chemical Engineering

Chalmers University of Technology

Abstract

The oxygen rich and relatively cold exhaust gases from fuel-efficient combustion engines bring challenges for the reductive aftertreatment of NO_x. In this context selective catalytic reduction over silver/alumina has shown positive results, especially with oxygenated reducing agents. In the present work, methanol, which is considered a promising renewable fuel, is evaluated as reducing agent for NO_x over supported silver catalysts. The aim is to gain increased understanding of the catalytic processes, especially focusing on low-temperature activity and selectivity. The role of the supported silver species is studied, together with the influence of the support material and the gas composition, including the formation of hydrogen. For this purpose model catalysts were prepared, characterized and evaluated in flow-reactor experiments.

The results show that the low-temperature activity for lean NO_x reduction with methanol over silver/alumina is highly dependent on the composition of supported silver species and their interplay with adsorbed and gas phase species. This work provides new insights in the role of small silver species for the selectivity to N₂ and the importance of somewhat larger silver species for catalytic activity at low temperature. These results were achieved by comparing silver/alumina samples of similar silver loading, but with different composition of silver species, as revealed by UV-vis spectroscopy, TEM and H₂-TPR. Furthermore, comparisons of different support materials during methanol-SCR conditions, show a higher NO_x reduction for silver supported on alumina than on ZSM-5. The NO_x reduction over the alumina based catalyst is found to improve when the C/N ratio is moderately increased. The influence of the silver loading was studied and the results show that sol-gel silver/alumina with 3 wt% silver gives a high NO_x reduction with methanol in a broad temperature interval, relevant for lean exhaust gases. Moreover, the observed formation of H₂ from methanol gives an indication of that the high low-temperature activity associated with oxygenated reducing agents may be connected to the abstraction of hydrogen from the oxygenate, studied here for methanol by DRIFT spectroscopy. One effect of hydrogen, observed in the present work by UV-vis spectroscopy, is reduction of silver species.

Keywords: silver/alumina; lean NO_x reduction; SCR, methanol; silver species; hydrogen; silver/ZSM-5

List of Publications

This thesis is based on the work presented in the following publications:

- I. Selective catalytic reduction of NO_x with methanol over supported silver catalysts**
Marika Männikkö, Magnus Skoglundh and Hanna Härelind Ingelsten
Applied Catalysis B: Environmental 119–120 (2012) 256– 266.
- II. Effect of silver loading on the lean NO_x reduction with methanol over Ag-Al₂O₃**
Marika Männikkö, Magnus Skoglundh and Hanna Härelind
Topics in Catalysis 56 (2013) 145-150.
- III. Methanol assisted lean NO_x reduction over Ag-Al₂O₃ - influence of hydrogen and silver loading**
Marika Männikkö, Magnus Skoglundh and Hanna Härelind
Accepted for publication in Topics in Catalysis (2015).
- IV. Role of hydrogen formation and silver phase for methanol-SCR over silver/alumina**
Marika Männikkö, Magnus Skoglundh and Hanna Härelind
Accepted for publication in Catalysis Today (2014).
- V. Silver/alumina for methanol-assisted lean NO_x reduction. Part 1 – on the influence of silver species**
Marika Männikkö, Xueting Wang, Magnus Skoglundh and Hanna Härelind
Submitted
- VI. Silver/alumina for methanol-assisted lean NO_x reduction. Part 2 – on the influence of reactions of methanol**
Marika Männikkö, Xueting Wang, Magnus Skoglundh and Hanna Härelind
Submitted

Contribution report

- I.** I prepared the catalysts, performed all experimental work, interpreted the results together with my co-authors, wrote the first draft of the manuscript and was responsible for writing and submitting the manuscript.

- II.** I prepared the catalysts, performed all experimental work, interpreted the results together with my co-authors, wrote the first draft of the manuscript and was responsible for writing and submitting the manuscript.

- III.** I performed all experimental work, interpreted the results together with my co-authors, wrote the first draft of the manuscript and was responsible for writing and submitting the manuscript.

- IV.** I performed all experimental work, interpreted the results together with my co-authors, wrote the first draft of the manuscript and was responsible for writing and submitting the manuscript.

- V.** I performed most of the experimental work, interpreted the results together with my co-authors, wrote the first draft of the manuscript and was responsible for writing and submitting the manuscript.

- VI.** I performed most of the experimental work, interpreted the results together with my co-authors, wrote the first draft of the manuscript and was responsible for writing and submitting the manuscript.

Contents

1. Introduction.....	1
1.1. Objectives.....	3
2. Hydrocarbon assisted selective catalytic reduction	5
2.1. Main principles.....	5
2.2. Challenges	6
2.3. Catalytic materials.....	7
2.4. Supported silver catalysts.....	8
2.4.1. The support.....	8
2.4.2. Ag/alumina	8
2.4.3. Ag-ZSM-5	9
2.4.4. The hydrogen effect.....	10
3. Methanol	13
3.1. Methanol fuel	13
3.2. Methanol as reducing agent for lean NO _x reduction.....	14
4. Experimental methods.....	15
4.1. Catalyst preparation.....	15
4.1.1. Sol-gel	16
4.1.2. Ion-exchange	16
4.1.3. Incipient wetness impregnation.....	16
4.1.4. Acid leaching.....	17
4.1.5. Microemulsion.....	17
4.1.6. Physical mixing	17
4.2. Catalyst characterization	18
4.2.1. BET - specific surface area.....	18
4.2.2. EDX - silver content.....	19
4.2.3. XRF – silver content.....	19
4.2.4. UV-vis spectroscopy - silver species.....	20
4.2.5. XPS – silver species	20
4.2.6. TEM – silver particle size.....	21
4.2.7. Temperature programmed desorption and reduction.....	21
4.2.8. DSC – adsorption of hydrogen	22
4.3. Catalytic performance	22
4.3.1. Flow reactor experiments	22
4.3.2. Fourier Transform Infrared (FTIR) spectroscopy.....	23
4.3.1. Mass spectrometry.....	24
5. Selective catalytic reduction with methanol	25
5.1. Influence of the support material	25
5.2. Influence of silver species	27
5.3. Influence of gas composition	39
5.4. Formation and influence of hydrogen	43

6. Concluding remarks	49
7. Outlook.....	51
Acknowledgements	52
References.....	53

List of abbreviations

Ag^+ , Ag_n^{m+}	Silver ion and silver cluster, consisting of a few silver atoms
$\text{Ag}/\text{Al}_2\text{O}_3$	Silver alumina
BET	Brunauer-Emmett-Teller, method for surface area determination
CH_3OH	Methanol
C/N	Number of carbon atoms per number of nitrogen atoms
CO	Carbon monoxide
CO_2	Carbon dioxide
DME	Dimethyl ether
DRIFTS	Diffuse reflectance infrared Fourier-transform spectroscopy
DSC	Differential scanning calorimetry
EDX	Energy Dispersive X-ray spectroscopy
FTIR	Fourier-transform infrared spectroscopy
HC	Hydrocarbon
H_2	Hydrogen
HC-SCR	Hydrocarbon assisted selective catalytic reduction
λ	Lambda, air/fuel ratio, ($\lambda = 1$ at stoichiometric air/fuel ratio)
LE	Sample prepared by leaching in nitric acid
ME	Sample prepared using microemulsion
MS	Mass spectrometry
MX	Sample prepared by physical mixing
N_2	Nitrogen
NCO	Isocyanate
NH_3	Ammonia
N_2O	Nitrous oxide, also called laughing gas
NO_x	Nitrogen oxides (NO and NO_2)
NSR	NO_x storage and reduction catalyst, also called LNT (Lean NO_x trap)
SCR	Selective catalytic reduction
SEM	Scanning electron microscopy
SG	Sample prepared according to sol-gel method
TEM	Transmission Electron Microscope
TPD	Temperature programmed desorption
TPR	Temperature programmed reduction
TWC	Three-way catalyst
UV-vis	Ultraviolet and visible light
XPS	X-ray photoelectron spectroscopy
XRF	X-ray fluorescence
ZSM-5	Zeolite named after Zeolite Socony Mobil, also called MFI

1. Introduction

Concerns for high anthropogenic carbon dioxide (CO₂) emissions and limited fossil fuel resources have resulted in a common interest in alternatives to the conventional otto engine, fuelled with petrol. Such alternatives are for example bio-fuels and more fuel-efficient engines, like combustion engines operated in excess oxygen, i.e. diesel and lean-burn engines. The greenhouse gas emission standards for passenger cars and light commercial vehicles in the European Union as well as the favourable tax system in some European countries are also driving forces for the successive transfer towards engines operating in oxygen excess [1]. In fact, today 50% of all new cars in Europe are driven by a diesel engine [2]. Diesel engines are in general more fuel efficient than petrol engines, but if driven in lean conditions the fuel efficiency for petrol engines can be improved with ca 15 – 30% [3-5] and thus less CO₂ is produced per driven kilometre, compared to conventional stoichiometric combustion.

A further reduction of CO₂ emissions can be achieved by using fuels derived from renewable sources. Ethanol, vegetable oil, biodiesel (esters), biogas, ETBE (etherized bioethanol), methanol and DME (dimethyl ether) are considered promising alternative fuels by the European Commission [6]. Methanol, which is studied as reducing agent in this thesis, is discussed as a potential renewable fuel for transports on road and at the sea [7]. Methanol can be used as fuel in stoichiometric conditions or in engines operating in oxygen excess. The latter is favourable owing to higher fuel-efficiency and thus lower CO₂ formation. At the same time, however, the high oxygen content in the exhaust gases is a challenge when it comes to reducing the nitrogen oxides (NO_x) emissions. This issue needs serious consideration since the transport sector is a large source of NO_x emissions. Of the NO_x emissions in the European Union in 2012 (Figure 1.1), 57% originated from transports, where road-transport contributed with 31% [8]. In diesel exhausts, NO_x and particulates are present in high amounts, while the emissions of carbon monoxide (CO) and unburned hydrocarbons are low [9]. The formation of NO_x and particulate matter are related in the sense that if the formation of one decreases, formation of the other is favoured [9]. Running an engine in conditions which produce more NO_x has been reported to result in fuel savings [10], why the need for efficient NO_x reduction in lean conditions is even more important.

The high temperature in internal combustion engines causes nitrogen and oxygen in the air to react and form NO_x. At ambient temperatures oxygen and nitrogen do not react with each other, but with increasing temperature the reaction rate of nitric oxide (NO) formation, according to the Zeldovich mechanism [11], increases exponentially. Subsequently, in the presence of excess oxygen, oxidation of NO to nitrogen dioxide (NO₂) occurs. NO_x from engine exhausts typically consists of a mixture of 95% NO and 5% NO₂ [11]. NO_x plays a major role in the photochemistry of the troposphere and stratosphere, where it catalyses ozone destruction. Other undesirable effects are acid rain and contribution to global photo-

oxidation pollution. Furthermore, NO_x is hazardous to human health by causing lung infections and respiratory allergies, like bronchitis and pneumonia [11].

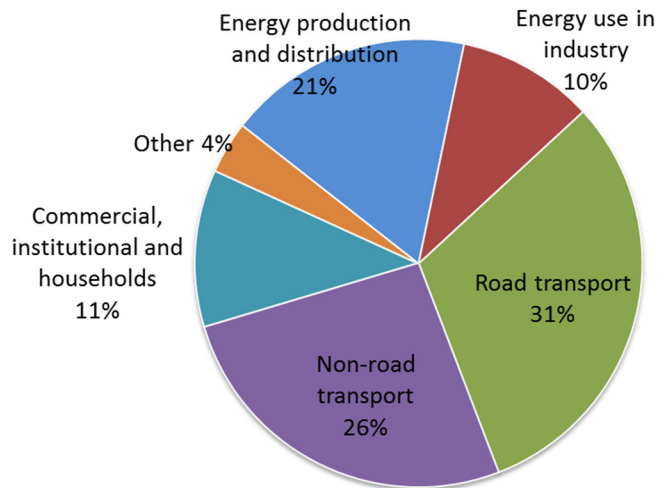


Figure 1.1. NO_x emissions in 28 countries in the European Union, 2012 [8].

The research in the area of lean NO_x after-treatment started in the early 1980's [3] and the first regulation comprising NO_x emissions (Euro I) was introduced in 1992 [12]. Since then the allowed emission levels have dramatically decreased, for example for heavy duty diesel engines from 8.0 to 0.4 g NO_x/kWh , in Euro VI, 2013 [13]. Until recently the NO_x emissions from diesel engines could be controlled by engine measures only. Now, however, the more stringent emissions legislation requires catalytic control [2]. In stoichiometrically operating petrol engines, with an air/fuel ratio close to $\lambda = 1$, the three-way catalyst (TWC) can simultaneously oxidize CO and hydrocarbons, and reduce NO_x . Diesel engines, however, operate at much higher air/fuel ratios, typically at $\lambda = 1.2 - 1.5$ at full loads, and at $\lambda = 10$ during idling [14]. At these high air-to-fuel ratios the TWC cannot efficiently reduce NO_x . Available catalytic techniques to reduce NO_x in lean conditions are lean NO_x traps (LNT), ammonia-assisted selective catalytic reduction ($\text{NH}_3\text{-SCR}$) and hydrocarbon-assisted selective catalytic reduction (HC-SCR). Lean NO_x traps, also called NO_x storage and reduction (NSR) catalysts, use a two stage cycle. During the lean stage the NO_x is stored on an alkali earth material (typically barium oxide or carbonate) as nitrates. When the engine is switched to fuel-rich conditions for a short period of time, hydrocarbons, hydrogen and CO in the exhaust gases reduce the nitrates over a rhodium component in the same way as in a TWC [2,10,11]. A disadvantage with the NSR catalysts, however, is their sensitiveness to sulphur [11,12]. Among $\text{NH}_3\text{-SCR}$ catalysts, on the other hand, more sulphur tolerant materials can be found, like vanadia and Fe-ZSM-5 [5,10]. $\text{NH}_3\text{-SCR}$ applications, however, require an on-board source of ammonia. Usually an aqueous urea solution is injected upstream of the SCR catalyst [2,10], where the high temperature of the

exhausts will hydrolyse urea to ammonia, which in turn will reduce the NO_x when it reaches the catalyst. The injection of urea can be effectively controlled to match the NO_x emissions at determined engine speed and load conditions [1]. Disadvantages with NH₃-SCR are, however, the possibility of unreacted ammonia escaping with the exhausts and the infrastructure needed for distribution of the urea solution [1,11,12]. These concerns resulted in the research on hydrocarbons as reducing agents in selective catalytic reduction of NO_x [11]. In HC-SCR applications the hydrocarbon based fuel is used as reducing agent. Thus, it gives advantages in the form of cost and user-friendliness, compared to NH₃-SCR. The main challenge for HC-SCR is, however, activity and selectivity at low temperatures [12].

The research on HC-SCR catalysts started in the 1980's with Cu ion-exchanged zeolites. Subsequently, many different materials have been studied, e.g. different cation exchanged zeolites and oxide-based catalysts [3]. Some of these are sensitive to water [11], while others have poor activity at low temperatures [12]. A promising system that has been subject to extensive studies is Ag/ γ -Al₂O₃ [1,12,15], which has shown good hydrothermal stability [16], is relatively inexpensive [17] and which low-temperature activity can be improved by addition of hydrogen [12].

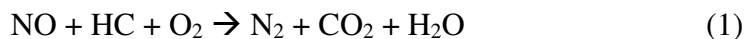
1.1. Objectives

The aim of this work is to gain increased understanding of lean NO_x reduction with methanol over supported silver catalysts. Special focus is given to low-temperature activity and selectivity, owing to the low temperatures of lean exhaust gases. Factors influencing the low-temperature performance are investigated, especially the role of the supported silver species (composition and loading), the influence of the support material and the gas composition, including the formation of hydrogen.

2. Hydrocarbon assisted selective catalytic reduction

2.1. *Main principles*

At ambient conditions the decomposition of nitrogen monoxide (NO) to nitrogen (N₂) and oxygen (O₂) is thermodynamically favoured, and should thus theoretically decompose. The decomposition reaction is, however, inhibited by its high activation energy (364 kJ/mol), but can be facilitated by a catalyst [18]. One feasible solution is hydrocarbon assisted selective catalytic reduction (HC-SCR), where the hydrocarbon-based fuel is used as reducing agent and injected into the exhaust system upstream of the catalyst. The reducing agent is needed since the unburned hydrocarbons and carbon monoxide (CO) in the exhausts of diesel and lean-burn engines are not present in high enough concentrations to reduce the nitrogen oxides (NO_x) [17]. In fact, the C1-to-NO_x molar ratio of the lean exhaust gases is below 0.1 [19]. Ideally during HC-SCR conditions, NO_x is selectively reduced in the catalytic reactions by the hydrocarbon (HC), forming nitrogen (N₂), carbon dioxide (CO₂) and water (H₂O). However, a competing reaction exists where the hydrocarbon (HC) non-selectively reacts with oxygen (O₂), i.e. combustion of the reducing agent occurs [4]. The combustion reaction is often predominant at high temperatures, but its reaction rate depends also on other factors, e.g. the catalytic material, the type of reductant, the C/N molar ratio and the oxygen content.



Simplified reactions during HC-SCR. (1) The NO_x reduction reaction. (2) Combustion of hydrocarbons.

Besides N₂, CO₂ and H₂O, also other reaction products are formed during HC-SCR. NO₂, N₂O, NH₃, CO and traces of hydrogen cyanide (HCN) are examples of bi-products reported for propene-SCR over Ag/Al₂O₃ [20]. NO₂ and NH₃ formation are often beneficial for the NO_x reduction, while the other bi-products mentioned are undesirable. N₂O, typically formed at temperatures below 300 °C, is of major concern owing to its high global warming potential [15]. In order to remove the unwanted bi-products an additional catalyst could be placed after the SCR catalyst [21]. Preferable is, however, selective formation of N₂ during the SCR process. Besides selectivity, other major aspects of SCR catalysts are to lower the reaction temperature and broaden the temperature window for catalytic activity [11].

2.2. Challenges

Achieving high activity and selectivity for HC-SCR catalysts in lean exhaust gases is challenging, owing to high oxygen concentrations, low temperatures, and exposure to water and sulphur. In addition, the catalysts should be durable and cheap to operate.

It is challenging to reduce NO_x under the strongly oxidizing conditions in exhaust gases from diesel and lean burn engines. The oxygen content varies from typically ca 18 - 20% during idling to only ca 3 - 5% during full-throttle operations [1], where the lower oxygen concentrations are still too high for a three-way catalyst to efficiently reduce NO_x . Lean NO_x reduction was reported by Tabata et al. [22] to be favoured to some extent by a higher oxygen concentration (5 - 18%) for methanol-SCR over Al_2O_3 , while Seker et al. [23] reported a slight negative effect on propene-SCR over $\text{Ag}/\text{Al}_2\text{O}_3$ when the oxygen concentration was increased from 5 to 20%. The effect is, however, small compared to for example the influence of temperature.

The relatively low temperatures of lean exhaust gases, compared to stoichiometric combustion, is a major concern for the efficient operation of HC-SCR catalysts. During normal operation of stoichiometric petrol engines the exhaust temperatures are typically in the range 400 - 800 °C [15]. For diesel engines in trucks the temperature is in general lower, ranging from 100 - 200 °C (during idling) up to ca 500 °C (during full-throttle operation). Light-duty diesel engines, usually operating at light load, typically have exhaust gas temperatures of ca 150 - 250 °C [1]. Twigg [2] compared exhaust gas temperatures during the European test cycle for the same type of car with a comparable petrol (1.6 l) and diesel engine (1.8 l), where the petrol engine resulted in exhaust temperatures of 300 – 700 °C and the diesel engine in 100 – 300 °C. This is in accordance with Klingstedt et al. [12], who reported on temperatures below 150 °C during ca 70% of the new European driving cycle (NEDC), for a cold-started $\text{Ag}/\text{alumina}$ catalyst during lean condition. The catalyst temperature is a major design challenge and depends on several factors, e.g. the engine size, the distance from the engine and other design parameters of the after-treatment system. Even if the formation of NO_x is more extensive at high engine temperatures, the relatively lower amount of NO_x formed at lower temperatures is not negligible when attempting to meet the current stringent emissions legislation. Thus, the SCR catalyst needs to be active also at the low exhaust gas temperatures, which follow the lower engine temperatures of lean operation compared to stoichiometric combustion.

An important aspect of HC-SCR catalysts are their durability, which is influenced by properties of the catalytic material as well as the operating conditions. Important material parameters are good thermal and hydrothermal stability and tolerance to sulphur. Conditions influencing the durability are high temperatures, the gas composition and exposure to metals and other elements, mainly from the lubricating oil, which could poison the catalyst surface. Today catalyst durability for heavy-duty applications is regulated by Euro VI, i.e. 160,000 – 700,000 km / 5 - 7 years depending on vehicle category [13].

The operating cost for HC-SCR applications is highly influenced by the consumption of the reducing agent, i.e. the fuel, and any hydrogen addition. In this respect it is important to limit the reductant feed, even though a high HC/NO_x ratio in general results in higher NO_x reduction [24]. However, too high HC/NO_x ratios may result in low selectivity to N₂, as in the study described in Paper II. Furthermore, Granger and Parvulescu [1] reported that the steadily supplied reductant, i.e. the diesel fuel, causes a fuel penalty of at least 3%. Kannisto et al. [24], on the other hand, calculated on a fuel penalty of 2% for diesel-SCR with a C/N molar ratio of ca 6 – 8 over a Ag/Al₂O₃ catalyst, including addition of 1000 ppm hydrogen. A comparable NO_x reduction by urea-SCR was reported to cause a cost equivalent to 0.5% fuel penalty [24]. Thus, it is important to keep the consumption of both reducing agent and hydrogen low, in order for HC-SCR to be a cost-effective alternative.

2.3. *Catalytic materials*

Several catalytic materials have been studied for lean NO_x applications, including supported noble metals, metal oxides, mixed metal oxides and zeolites [1]. The first studies in the early 1980's focused on Cu and other cat-ion exchanged zeolites. Cu exchanged mordenite showed good NO_x conversion at low temperature, but poor activity in the presence of water [3]. This led to the more water tolerant Cu-ZSM-5, which was discovered independently by Iwamoto et al. [25] and Held et al. [26] in 1990. High temperature in combination with water is, however, a major problem for zeolites, which typically decompose at temperatures above 700 °C. They can also be deactivated by dealumination, which causes cat-ions to convert into inactive oxides, or lose their crystalline structure, which is important for retaining high activity [19]. Another type of catalysts studied for lean NO_x applications are supported noble metals, where supported Pt has gained specific interest. Supported Pt catalysts show high tolerance to sulphur (SO_x) and water vapour, at the same time as they are active at lower temperature (< 300 °C) compared to Cu-ZSM-5 [11,19]. Disadvantages of supported Pt catalysts are, however, a narrow temperature interval for NO_x reduction and poor selectivity, producing large amounts of N₂O [3,11]. Supported gold catalysts were reported to show better selectivity compared to Pt, but poor low-temperature activity [27]. A less expensive alternative are metal oxide based catalysts. Several base metal oxides and metals (e.g. Al₂O₃, TiO₂, ZrO₂, MgO promoted by Co, Ni, Cu, Fe, Sn, Ga, In or Ag) are active for lean NO_x reduction with hydrocarbons [15,27]. Metal oxides show promising results in the form of high stability and tolerance to SO_x and water vapour [11], where silver has gained special interest since silver-based formulations are among the most active and selective [15]. In the following section, 2.4, a more detailed description of silver supported on alumina and ZSM-5 is given.

2.4. *Supported silver catalysts*

2.4.1. **The support**

The purpose of the support material in catalysis is to provide a large surface area, reduce sintering of the active phase and possibly to participate in the reaction. Alumina is the most common support in catalysis owing to its excellent thermal and mechanical stability and its rich chemistry [28]. Of the different forms of alumina, the porous amorphous γ - Al_2O_3 is the most widely used, by itself or with metals incorporated in the structure. Alumina is prepared from $\text{Al}(\text{OH})_3$ (Bayerite or Gibbsite) or AlOOH (Böhmite) by dehydration. In order to produce the high surface area (50 – 300 m^2/g) of γ - Al_2O_3 the calcination temperature should be 500 - 850 °C. If this temperature is exceeded the alumina is transformed to another structure, for example above 1150 °C α - Al_2O_3 with a surface area of only 1 - 5 m^2/g is formed. γ - Al_2O_3 shows high thermal stability and contains many hydroxyl groups on its surface (10 – 15 per nm^2), forming Brønstedt acids (proton donors) and Brønstedt bases (proton acceptors) [28]. Brønstedt acids can be converted to Lewis acids (electron pair acceptors) by loss of water.

Another support material often used in catalysis is zeolites, i.e. microporous, crystalline aluminosilicates [28]. The zeolite structure is an open framework and contains an extensive network of channels and cages, where atoms or molecules can adsorb and react. Zeolites are prepared by hydrothermal synthesis in autoclaves from structure directing agents, like tetramethylammonium. Their porous structure, acidity and the possibility to exchange existing cat-ions (metals, NH_4^+ or H^+) makes zeolites interesting catalytic support materials. A wide variety of structures exist, all linking together SiO_4 and AlO_4 tetrahedra through their corner oxygen atoms [29]. ZSM-5 (also called MFI), used in the present work, has a two-dimensional structure, consisting of straight and sinusoidal channels (diameter 0.55 nm) perpendicular to each other and typically has Si/Al ratios ≥ 10 [28]. The Si/Al ratio determines the number of cat-ions in the structure, since the cat-ions are needed to compensate for the net charge of -1 of the aluminium (Al^{3+}) atom, compared to the silicon (Si^{4+}) atom. In its H-form the zeolite is a solid acid with Brønstedt acid (proton donor) sites, where the acidity depends on the surrounding of the proton [28]. In the same way as for alumina, Brønstedt acid sites can be converted to Lewis acid (electron pair acceptors) sites after loss of water.

2.4.2. **Ag/alumina**

In 1993, Miyadera [30] reported on high activity for lean NO_x reduction over $\text{Ag}/\text{Al}_2\text{O}_3$ in the presence of water. This was a major improvement compared to many of the previously studied catalysts, like Cu-ZSM-5, which has low hydrothermal stability. Tolerance to water is an important property of a catalyst, as water vapour is always present in exhaust gases. Since then numerous studies have been published on the subject of $\text{Ag}/\text{Al}_2\text{O}_3$ [9,15,17,20,24,31-47]. $\text{Ag}/\text{Al}_2\text{O}_3$ is made by basically two different categories of

preparation methods. One type results in silver on the catalyst surface, like conventional impregnation [30,35-37,47-50], incipient wetness impregnation [20,33-35,51-55] and microemulsion [56,57]. The other methods result in silver incorporated in the alumina matrix, like the sol-gel method [23,24,39-41,58,59], co-gelation [42,60] and co-precipitation [23]. It is generally accepted that the preparation methods resulting in silver incorporated in the alumina matrix gives a high dispersion of small silver species, while the impregnation methods result in somewhat lower dispersion. The dispersion is also influenced by the silver loading, i.e. a higher loading results in lower dispersion and vice versa. This is also reflected in the optimal silver loading reported for different preparation methods. For Ag/Al₂O₃ prepared by impregnation, the optimal silver loading is typically 2 – 3 wt% [30,33-36,38,47,49-53,61,62], while sol-gel samples usually show best NO_x reduction performance at a somewhat higher silver loading, ca 3 - 4 wt% [23,24,39-42,58-60]. Ag/Al₂O₃ prepared by the sol-gel method has been reported to show good thermal stability [23], is active in a broader temperature interval [23,39], at lower temperature [41,40], compared to when impregnation is used. These properties could be related to the support material and/or to the dispersion and oxidation state of silver on the catalyst surface. It has been proposed that the NO_x reduction over Ag/Al₂O₃ occurs mainly over small oxidized silver species, like silver ions and small oxidized silver clusters (Ag_n^{δ+}) [33]. Metallic silver particles are thought to cause combustion of the reducing agent, but might also play a role in the NO_x reduction mechanism, possibly by promoting oxidation of NO to NO₂ [46]. Accordingly, it has been suggested that an optimal surface Ag⁰/Ag⁺ ratio is needed in order to achieve a high NO_x reduction [46,53]. Another parameter influencing the catalytic performance is the choice of reducing agent. High activity for lean NO_x reduction over Ag/Al₂O₃ is reported for several reducing agents, both hydrocarbons and oxygenated compounds [30,41,52,53]. Miyadera [30] found higher NO_x reduction activity over Ag/Al₂O₃ with oxygenated compounds, like ethanol, compared to propene, when water was present. In the studies of Ag/Al₂O₃ by Kameoka et al. [63] and da Silva et al. [56] ethanol resulted in improved NO_x reduction performance compared to propene, at low temperatures (< 350 and 500 °C, respectively). However, at even lower temperatures, i.e. below 300 °C, Ag/Al₂O₃ is known to have poor activity [11], but it can be improved by the addition of hydrogen to the exhaust stream. The effect of hydrogen is discussed in section 2.4.4 below.

2.4.3. Ag-ZSM-5

A common method to introduce metal ions into zeolite structures is by ion-exchange, but also impregnation is used. Several metal ion-exchanged and impregnated zeolites have been identified as active for lean NO_x reduction, including Cu, Co, Ni, Mn, In, Ga, Pd and Ag, supported on e.g. ZSM-5, ferrite and mordenite. Some have shown low stability in the presence of water vapour (Cu, Co, In, Ga on ZSM-5) and others are reported to be active only at high temperature (Mn-ZSM-5 for CH₄-SCR) [64]. Seijger et al. [65] found that Ag-ZSM-5 (3.35 wt% Ag) was active for lean NO_x reduction with propene at relatively low temperature (maximum conversion at 275 °C). However, its activity was ranked low

compared to other silver zeolites; Ag-Na-BEA > Ag-H-FER, Ag-H-BEA, Ag-K-FER > Ag-H-ZSM-5. Besides the support material the catalytic activity is also dependent for example on properties of the silver (loading, dispersion and composition of Ag species) and the reductant (type and concentration). In addition to the above mentioned propene, several other reducing agents have been tested in HC-SCR over Ag-ZSM-5. Sato et al. [66] reported on Ag-ZSM-5 being active for lean NO_x reduction with ethane at high temperature (450 - 600 °C). Propene, DME and methanol was investigated as reducing agents for lean NO_x reduction by Masuda et al. [31], who found a poor activity for the reaction over Ag-ZSM-5, compared to Ag/mordenite and Ag/Al₂O₃. The reason for introducing a metal ion onto a catalyst surface is often to enhance low-temperature activity. Shi et al. [67], for example showed that the activity for lean NO_x reduction with methane started at lower temperature for a H-ZSM-5 catalyst impregnated with Ag, compared to a H-ZSM-5 catalyst. Like for alumina based silver catalysts, the silver supported on ZSM-5 can exist in different forms, i.e. mainly isolated silver ions, small silver clusters and larger agglomerates. Konova et al. [44] detected non-isolated Ag²⁺ ions (most probably small silver clusters, (Ag²⁺)_n) by electron paramagnetic resonance (EPR) spectroscopy on Ag-ZSM-5 prepared by impregnation, while ion-exchange resulted in both isolated and non-isolated Ag²⁺ ions. Bartolomeu et al. [68] used H₂-TPR, UV-vis spectroscopy and HR-TEM to study Ag-ZSM-5 (ion-exchange, 4.4 wt% Ag), and reported on the presence of Ag⁺ ions, partially charged silver clusters (Ag_n^{δ+}) and Ag⁰ particles with a mean diameter of 2.5 nm. Shi et al. [69] pointed on the influence of pre-treatment on the silver species formed. In a fresh Ag-ZSM-5 (ion-exchange, 9 wt% Ag) sample only isolated silver ions were observed by UV-vis spectroscopy, while samples thermally treated (500 °C, 1h) in a He stream also showed, besides the isolated silver ions evidence of small silver clusters and metallic silver particles. On the other hand, when a Ag-ZSM-5 sample was treated in an oxidative atmosphere (500 °C, 1h, 30% O₂ in He) no silver clusters or metallic particles were detected. Instead the silver was thought to be present as mixed oxides of amorphous character. The pretreatment in the inert gas resulted in high activity, but poor selectivity to N₂, while the oxidative pretreatment resulted in high selectivity, but low activity. Shibata et al. [70,71] investigated the influence of hydrogen addition on C₃H₈-SCR and found an enhanced low temperature activity over Ag-ZSM-5 (= Ag-MFI), likely owing to agglomeration of Ag⁺ ions to small silver clusters Ag_n^{δ+}, which in turn were suggested to promote partial oxidation of C₃H₈.

2.4.4. The hydrogen effect

Satokawa [72] first reported on significantly improved low-temperature activity for lean NO_x reduction by propane over Ag/Al₂O₃ by the addition of hydrogen (H₂) to the gas stream. Later the H₂ effect has been observed over Ag/Al₂O₃ for several reducing agents, like methane, ethane, propene, iso-butane [73], hexane [55], octane, toluene, methylcyclohexane, cyclohexane [74], butanol, butanone [3] and ethanol [75]. The enhancement for oxygenated reducing agents is, however, significantly smaller than for hydrocarbons [3,76]. The promoting effect of hydrogen is reversible, i.e. the NO_x reduction

decreases when hydrogen is removed from the flow, but increases again as soon as hydrogen is switched in [77]. The introduction of hydrogen can be repeated several times without loss of catalytic activity. The effect seems to be limited to silver catalysts, where the support materials alumina and ZSM-5 has shown most promising results [1]. The reasons behind the positive effect of hydrogen are still under debate and several explanations have been suggested; influence of the chemical state of silver [59,78,79], removal of reaction inhibitors from the catalyst surface [79-82], partial oxidation of the reducing agent [43,78,83], formation of reactive species which can readily reduce NO_x [43,82,84,85] and formation of hydroperoxy and hydroxyl radical species [43]. Partial oxidation of hydrocarbons is thought to be an important step in the mechanism. Shimizu et al. [86] suggested that H_2 causes Ag^+ ions to form small Ag hydride clusters (HAg_4H). Subsequently O_2 reacts with the clusters, forming hydrogen peroxide-like species, which in turn activates the hydrocarbons by partial oxidation to surface oxygenates. Brosius et al. [79], on the other hand, proposed that the promotional effect of H_2 occurs via partial oxidation of hydrocarbons over Ag^0 , formed from surface AgNO_3 reduced by H_2 . Also Kannisto et al. [80] proposed that an important role of H_2 is the reduction of surface nitrates, which could inhibit the HC-SCR reaction. Other surface species, like -NCO are, however, thought to enhance the reduction of NO_x . Wichterlova et al. [84] found that the addition of H_2 results in a remarkable increase in the number and variety of surface species, like -NCO on Al sites, and proposed that H_2 participates directly in the reaction mechanism. Finally, it should be considered as pointed out by Breen and Burch [77], that it is probable that all the suggested reasons listed above, can contribute and that it very much depends on the reaction conditions as to which one is most important.

3. Methanol

3.1. *Methanol fuel*

Currently methanol is mainly produced from fossil sources, i.e. from syngas ($\text{CO} + \text{H}_2$) produced by catalytic reforming of natural gas and coal [87]. However, methanol can also be produced from renewable sources, like wood, black liquor, agricultural biomass, waste biomass and sewage sludge. In fact, methanol can be derived from any material that can be decomposed into CO or CO_2 and hydrogen [7].

The use of alcohols (methanol and ethanol) as transportation fuel started already at the time of invention of the internal combustion engine (ICE) [7]. In the beginning of the twentieth century competitions were held between alcohol and petrol driven vehicles and the debate was lively about which fuel resulted in the best performance. Reasons for petrol finally becoming the dominating fuel were lower cost, local alcohol politics, the need for alcohol as raw material for other products, etc. Several times during the history alcohol fuel has, however, regained attention. Germany, for example, was interested in becoming independent of oil during the World War II and California, starting from the 1970's, wanted to reduce its air pollution by introducing methanol fuel. The methanol-petrol blend M85 has been used in California with a peak of 20,000 flexi-fuel vehicles in 1997. Compared to pure petrol, methanol fuel was found to be cheaper, extend the life-time of the engine and decrease the exhaust emissions [7]. Also in China methanol-petrol blends are used. Taxis and busses run on fuel with high methanol content (M85 to M100), while retail pumps sell fuel with 15% methanol (M15) or less in many parts of the country [88]. In Europe methanol is considered as one of several promising future bio-fuels for the transport sector [6]. In addition methanol has recently been introduced as a maritime fuel [89,90].

Methanol can be used as fuel in spark ignition engines (SI) as well as in compression ignition (CI) engines [7]. Beneficial for the use in SI engines is the high octane rating of methanol, which results in more power compared to petrol. A problem, on the other hand, is that methanol is difficult to ignite at low temperatures. This can be solved by adding small amounts of petrol (ca 15%), which is miscible with methanol in all proportions. Blends containing more than 10% methanol requires minor modifications of the engine, and result in higher efficiency. Thus, despite the lower energy content of methanol (ca 50%) compared to petrol, less than the expected double amount of methanol is consumed. Also compared to diesel fuel, methanol has lower energy content; hence larger fuel tanks might be needed when methanol is used as fuel. On the contrary to methanol-petrol blends, additives are required for methanol to blend with diesel. Also the problem with the low cetane number of methanol can be solved by additives in methanol-diesel blends. However, for ignition of pure methanol in a CI engine, sparkplugs or glow plugs are required [7]. Using methanol, as compared to diesel, as fuel for CI engines gives an advantage in form of lower formation of smoke, soot and particles [7]. Reports on NO_x formation are,

however, contradictory. Brusstar et al. [91], Seko et al. [92] and Udaymar et al. [93] report on low NO_x emissions when methanol fuel is used, compared to diesel. Sayin et al. [87] and Huang et al. [94] report on increased NO_x formation with increasing methanol content in methanol-diesel blends, while Song et al. [95] observed the opposite. As discussed in section 1, the formation of NO_x emissions is highly dependent on the combustion temperature, where the peak temperature is of particular importance. The lower cetane number of methanol, compared to diesel, contributes to a higher peak temperature in the cylinder, while its lower heating value and higher latent heat of vaporization, act contradictory [87]. Besides the methanol content of the fuel, the combustion temperature is influenced by many other parameters, like the engine speed and load, and ignition timing [92]. It is difficult to compare different studies, but obviously some condition reduce the NO_x formation when using methanol or methanol-diesel blends, as compared to pure diesel.

3.2. Methanol as reducing agent for lean NO_x reduction

The lean NO_x reduction with methanol over silver supported on alumina often results in low NO_x reduction, compared to when ethanol is used as reductant [30,48,63]. Remarkably high NO_x reduction with methanol over Ag/Al₂O₃ prepared by the sol-gel method is, however, reported by Zhu et al. [96]. In fact, the maximum NO_x reduction with methanol as reducing agent was similar as for ethanol, even though methanol was fed at a lower C/N ratio compared to ethanol. Masuda et al. [31] compared the lean NO_x reduction over silver supported on different materials. When methanol was used as reductant, Ag/ZSM-5 showed a poor NO_x reduction performance compared to Ag/Al₂O₃. Methanol was concluded to be a suitable reducing agent over Ag/Al₂O₃ in at ca 350 - 450 °C. Compared to γ-Al₂O₃, methanol-SCR over Ag/Al₂O₃ (3 wt% Ag, impregnation) resulted in slightly higher NO_x reduction activity at somewhat lower temperature [31]. Kameoka et al. [63], found at high temperatures lower NO_x reduction with methanol over Ag/Al₂O₃ compared to γ-Al₂O₃. At low temperatures (250 °C), however, the NO_x reduction was low, but higher for the silver containing catalyst compared to γ-Al₂O₃. Tamm et al. [97], on the other hand, found no significant difference in maximum NO_x reduction over Ag/Al₂O₃, compared to γ-Al₂O₃. All three above mentioned studies [31,63,97] show that the lean NO_x reduction with methanol occurs at lower temperature over Ag/Al₂O₃ compared to γ-Al₂O₃.

HC-SCR reactions over Ag/Al₂O₃ has been studied by Wu et al. [48] and He et al. [17] with methanol and several other reducing agents. He et al. [17] suggested a reaction mechanism for C1 reductants, with intermediates including formates, NO₂ and nitrates. The reason for the low NO_x reduction with methanol was suggested to be the low reactivity of these intermediate surface species in forming –NCO species [17]. Similar species were observed by Tamm et al. [98] during DME-SCR and methanol-SCR over γ-Al₂O₃, where formohydroxamic acid and –NCO species were suggested to be important intermediates. The authors proposed that a partly similar reaction mechanism is operational for DME-SCR over γ-Al₂O₃ as for HC-SCR over Ag/Al₂O₃ [98].

4. Experimental methods

In this work, supported silver catalysts are evaluated as catalysts for lean NO_x reduction with methanol, focusing on the influence of temperature, gas phase composition and the supported silver species. Powder samples were prepared and coated onto cordierite monoliths. The monolith samples were used in flow reactor experiments, BET measurements, NH₃-TPD and NO-TPD. The powder samples were analysed with regards to specific surface area (BET) and silver content (SEM/EDX and XRF), and the silver species were characterized by UV-vis spectroscopy, XPS, TEM and H₂-TPR.

4.1. Catalyst preparation

The Ag/Al₂O₃ samples, used in Paper I - IV, were prepared according to the sol-gel method including freeze-drying, described in detail by Kannisto et al. [41]. AgNO₃ was used as silver precursor and aluminium isopropoxide (AIP) as precursor for γ -Al₂O₃. ZSM-5 based catalysts (H-ZSM-5, Ag/H-ZSM-5, Pd/Ag/H-ZSM-5) were studied in Paper I. Zeolite H-ZSM-5 powder (Akzo Nobel Catalysts BV) with a SiO₂/Al₂O₃ molar ratio of 40 was used for the preparation of Ag/H-ZSM-5 by ion-exchange. Part of the prepared Ag/H-ZSM-5 sample was subsequently used to prepare Pd/Ag/H-ZSM-5 by incipient wetness impregnation. Ag/Al₂O₃ samples with different composition of silver species were studied in Paper V and VI. Besides the above mentioned sol-gel method, samples were prepared by acid leaching, microemulsion and physical mixing. The acid leaching was carried out on Ag/Al₂O₃ samples prepared by the sol-gel method, where small silver species were removed by leaching in a solution of nitric acid. During the microemulsion preparation method silver particles were prepared in a water-in-oil microemulsion, where the continuous oil phase consisted of n-heptane with Brij L4 as surfactant. AgNO₃ in an aqueous solution was used as silver precursor. The physically mixed samples were prepared by grinding γ -Al₂O₃ and Ag₂O in a mortar, followed by calcination. More detailed descriptions of the catalyst sample preparation can be found in Paper I and V.

For the flow reactor experiments the powder samples were deposited on cordierite monolith substrates (Corning, 400 cpsi, 188 channels). For each sample, a slurry was prepared by mixing the powder sample with a binder at a weight ratio of 80:20 in Milli-Q water. The binders used were Bindzil (30NH₃/220, Colloidal Silica, Akzo Nobel, Eka Chemicals) and Disperal P2 (Sasol) for the ZSM-5 and γ -Al₂O₃ based samples, respectively. The monoliths were immersed in the wash-coat slurry, dried (90 °C, 5 min) and calcined (550 °C, 2 min). The procedure was repeated until the weight of the wash-coat was 0.5 g, corresponding to ca 20% of the final dry monolith sample weight. The monolith samples were finally calcined in air at 550 °C for 2 h and at 600 °C for 2 h and 3 h, for the zeolite based, Al₂O₃ and Ag/Al₂O₃ samples, respectively.

4.1.1. Sol-gel

The sol-gel process involves formation of a sol followed by transformation into a gel. A sol comprises small particles (1 nm – 1 μ m) prevented from sedimentation by Brownian motion of the solvent molecules. These small particles can be obtained from a precursor, such as an inorganic salt or a metal alkoxide, by hydrolysis and partial condensation [99]. A solvent (typically water or an alcohol) and acid or base is added to the precursor to facilitate the hydrolysis and the condensation process. When a sol is formed, catalytically active metal ions can be added and allow to adsorb on the small particles. The subsequent removal of excess solvent, results in a three-dimensional network between the particles encapsulating the solvent, i.e. a gel is formed. As this highly porous structure is desirable in catalysis, the subsequent drying should be performed slowly (preferably by freeze-drying) and the temperature should be increased slowly up to the calcination temperature. Preservation of the structure ensures, besides a large surface area, a high dispersion of the added metal ions throughout the support matrix.

4.1.2. Ion-exchange

In an ion-exchange process an ion interacting with the surface of the support is replaced with another ion [99]. The support is exposed to a large volume (compared to the pore volume) of a solvent containing the ion to be introduced on the surface of the support. The ions from the solvent gradually diffuse into the pores and replace the ions of the support, which in turn diffuse into the solvent bulk. During ion-exchange for zeolites typically cations, e.g. H^+ , Na^+ or NH_4^+ bonded to the zeolite framework, are exchanged with metal cations in a solution. The cat-ions are coordinated to the negatively charged AlO_4 tetrahedrons in the zeolite structure [99], why the Si/Al ratio of the zeolite is of importance for the resulting metal loading and dispersion. After the ion-exchange has reached equilibrium, the solvent containing the exchanged cat-ions is removed and the sample is washed a few times with clean solvent in order to remove all exchanged ions. Finally, ion-exchanged zeolites prepared as catalysts are dried and calcined, fixating the introduced ions to the support matrix.

4.1.3. Incipient wetness impregnation

In incipient wetness impregnation (also called dry impregnation or capillary impregnation) the dry catalyst powder is mixed with only enough solution, containing the active phase precursor, to fill the pores of the support [100]. The volume of liquid needed to reach the stage, when the solid mixture turns into a viscous liquid, is determined by slowly adding small weighed quantities of the solvent to a weighted amount of the dry support. By the incipient wetness impregnation method a desired metal loading can be achieved since all the active metal added to the support is expected to remain on the catalyst surface, unlike during conventional impregnation when an excess of solvent is used and later removed. Finally, the catalyst powder is dried and calcined.

4.1.4. Acid leaching

Leaching is used in hydrometallurgy when recovering silver from various kinds of ores and has also been investigated as a method for recovery of silver from spent Ag/ α -Al₂O₃ catalysts [101]. The leaching is affected by the type of lixiviant chosen, the reaction temperature, the ratio of solid and liquid, and the stirring speed [101]. Acid leaching can, however, also be used in order to tailor the composition of silver species during catalyst preparation. When Ag/Al₂O₃ is exposed to nitric acid weakly bound, i.e. mainly large, silver species/particles are removed from the catalyst surface [42]. The leaching is performed by immersing Ag/Al₂O₃ powder in an aqueous nitric acid (HNO₃) solution. After vigorous stirring during the leaching process, excess solvent is removed and the sample is washed several times in order to remove the silver species/particles transferred to the solvent. Finally, the sample is dried and calcined.

4.1.5. Microemulsion

Metallic nanoparticles can be created using water-in-oil microemulsions [102]. One possible route is by mixing an aqueous solution of a metal precursor (often a salt) with an organic solvent and a surfactant. The surfactant molecules will self-assemble with the polar hydrophilic head towards the water solution and the hydrophobic hydrocarbon chain towards the oil phase [103]. The proportion of water, oil and surfactant, and the choice of surfactant are important for achieving a water-in-oil microemulsion [103]. In water-in-oil microemulsions the surfactant forms so called reversed micelles around the water droplets, where the size of the reversed micelles increases with the amount of water added [103]. This also to some extent controls the size of the metal nanoparticles formed in the water droplets [102]. The metal nanoparticles are formed by reduction of the metal ions (formed when the metal precursor is dissolved) inside the water droplets. The reduction can be accomplished by part of the surfactant molecule acting as reducing agent. In order to create a heterogeneous catalyst the nanoparticles need to be deposited onto a carrier material, like γ -Al₂O₃. One way to achieve this is to use a solvent, like tetrahydrofuran (THF), that dissolves the surfactant and is miscible with both water and oil [102]. The process is carried out during vigorous stirring after addition of the catalyst support material and the solvent. In order to achieve an even distribution of the metal particles on the support, care has to be taken not to add THF too fast, which could cause extensive agglomeration of the particles [102]. When the surfactant is dissolved the formed nanoparticles will precipitate, where after the catalyst powder (including the deposited metal particles) is filtered off. The remaining surfactant is removed by washing with more solvent. Finally, the catalyst powder is dried and calcined.

4.1.6. Physical mixing

Catalytic material can be prepared by physically mixing two solids. For zeolites solid-state ion-exchange is used for introducing desired ions into the zeolite structure. However, also

oxide based catalysts can be prepared by mixing two solids. Here the reaction interface in the powder mixture consists of intergranular contact points between the solid substrate and the other solid product [104]. The migration of one solid over the surface of the other solid is an important factor for achieving a high dispersion [104]. The dispersion can be further increased by ball-milling, where the milling time is important [105]. By mechanical force, milling increases the surface area of solids and the area of regions where the solids are in close contact and can react with each other [105]. However, if the grinding is not extensive, i.e. milling is not used, likely a low dispersion is achieved where metal particles are mainly deposited on the outer surface of the support, rather than inside the pores. When a mixture of silver oxide and alumina is calcined at high temperature silver is deposited on the alumina surface.

4.2. Catalyst characterization

4.2.1. BET - specific surface area

The specific surface area can be measured by the BET method, named after Brunauer, Emmett and Teller who first published the theory behind the BET method in 1938 [106]. Before the measurement the sample is evacuated during heating, while adsorbed contaminants (i.e. mainly water) are removed. The sample is then cooled under vacuum, usually with liquid nitrogen to 77 K. An inert gas, like nitrogen, is dosed in small quantities onto the sample. After each dose the pressure (P) is allowed to equilibrate and the adsorbed volume (V) of the inert gas is calculated by the ideal gas law. The adsorbed inert gas is gradually building up a monolayer and the number of molecules forming the monolayer is determined. As the surface area occupied by one molecule of the inert gas at a specified temperature is known (one N₂ molecule occupies 0.162 nm² at 77 K) the total surface area can be calculated [107]. At low partial pressures the relationship between P/V(P₀-P) and P/P₀ is linear. By plotting these for each of the dosing steps mentioned above, V_m can be determined from the slope and the intercept of the curve.

$$\frac{P}{V(P_0 - P)} = \frac{1}{V_m C} + \frac{C - 1}{V_m C} \frac{P}{P_0}$$

P = partial pressure of inert gas at equilibrium

V = volume adsorbed gas at P

P₀ = saturation pressure of the inert gas at the experimental temperature

V_m = volume of inert gas forming a monolayer

C = a constant

In this work the BET method was used to determine the specific surface area of the samples, using a Micromeritics Tristar 3000 instrument for the powder samples (Paper I, II and V) and a Micromeritics ASAP 2010 instrument for the monolith samples (Paper I).

4.2.2. EDX - silver content

Energy dispersive X-ray spectroscopy (EDX) can be used to analyse the chemical composition of a catalyst. In this technique, illustrated in Figure 4.1, the sample is radiated with an electron beam, which excites electrons in the inner electron shells of the sample atoms. When an excited electron leaves the atom it creates an electron hole, which is filled with an electron from a higher electron shell. This results in an emitted X-ray, corresponding to the energy difference between the two electron shells. The energy of the X-ray is measured and since it is characteristic for the element, the elemental composition of the sample can be determined [108].

The silver content in the Ag/H-ZSM-5 and Pd/Ag/H-ZSM-5 powder samples in Paper I was analysed by an EDX (Oxford Inca EDX system) connected to a scanning electron microscope (Leo Ultra 55 FEG SEM) and found to be 5 wt%. Since the nominal content of Pd was very low (0.01 wt%) in the Pd/Ag/H-ZSM-5 sample, the Pd content was not possible to analyse.

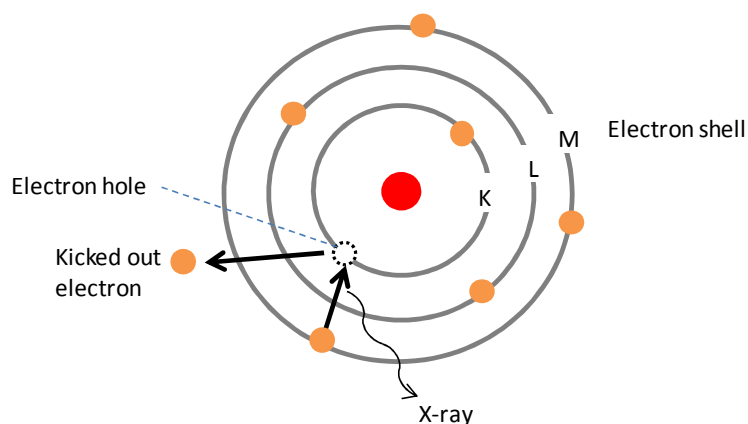


Figure 4.1. An electron hole is created when an electron is kicked out by the incident electron beam. When the electron hole is filled by an electron from an outer shell, an X-ray is emitted.

4.2.3. XRF – silver content

X-ray fluorescence (XRF) spectroscopy can be used for elemental analysis. When the sample is placed in a beam of high energy X-rays the atoms absorbing the X-rays become excited and emit X-rays of characteristic wavelength [109]. By measuring the wavelength and intensity qualitative and quantitative analyses can be performed [109]. For qualitative measurements the angle of diffraction θ is measured, from which the wavelengths of fluorescence λ can be calculated using the Bragg equation ($n\lambda = 2d \sin\theta$, where d is the spacing between the crystal layers). The intensity of fluorescence is independent of the chemical state of the element, why sample preparation often is not needed.

The silver content in Ag/Al₂O₃ was analysed by XRF (PANalytical PW2424) in Paper V.

4.2.4. UV-vis spectroscopy - silver species

UV-vis diffuse reflectance spectroscopy can be used to analyse the chemical composition of a sample. This technique is based on the ability of atoms to absorb only discrete amounts of energy, corresponding to the energy required to move an electron from a lower energy level to a higher energy level [109,110]. For molecules, however, the transfers in electronic energy levels are superimposed by transitions in vibrational and rotational energy levels, causing broadening of the otherwise narrow and highly characteristic absorption bands. On the other hand, molecular spectroscopy can provide detailed information on molecular structure and chemical properties [109]. The sample is irradiated with light in the ultraviolet (200 – 400 nm) and visible (400 – 800 nm) wavelength region, while the absorbance is measured as a function of wavelength. For species bound to the catalyst surface the surrounding support material will influence the spectrum, by influencing the absorption wavelengths of the studied surface species and possibly by interfering absorption of the support material. To correct for the latter, a spectrum of pure support material could be subtracted from the spectrum of the studied sample.

In this work UV-vis diffuse reflectance spectroscopy was performed to characterize silver species in the powder samples (H-ZSM-5, Ag/H-ZSM-5, γ -Al₂O₃ and Ag/Al₂O₃) in Paper I, IV and V. A Varian Cary 5000 UV-vis-NIR spectrophotometer, with Labsphere Spectralon as reference, was used.

4.2.5. XPS – silver species

X-ray photoelectron spectroscopy (XPS) can be used for analysing the surface composition, the oxidation state and chemical environment of species on the surface (ca 0 – 10 nm) of solid materials [111,112]. X-rays are used to create highly excited ions by detaching electrons from the inner (core) electron shells [109]. The kinetic energy distribution of the emitted photoelectrons is measured, resulting in a photoelectron spectrum [111]. An element can be identified by its characteristic set of peaks, dependent on a characteristic binding energy (BE) for each core orbital and the incident photon energy [111,112]. Changes in the oxidation state or the environment of the element, however, causes small shifts for the peaks in the spectrum, called chemical shifts. The chemical shifts can be used to distinguish between different oxidation states and chemical environments for an element [111]. Electrically insulating samples may, however, charge up during measurement. The positive charge creates an equal shift for all XPS peaks towards higher binding energies. This can be compensated for by correcting against the binding energy of a known peak, for example the binding energy of C1s (284.6 eV) [28].

In this work XPS (Physical Electronics Quantum 2000 scanning ESCA microprobe with an Al K α , 1486.6 eV, X-ray source) was used to characterize the silver species on the surface of Ag/Al₂O₃ in Paper III.

4.2.6. TEM – silver particle size

The size and shape of nanoparticles can be studied using transmission electron microscopy (TEM). A TEM instrument is similar to an optical microscope, but gives a higher resolution and uses electromagnetic lenses instead of optical lenses [28]. The thin sample is radiated with a high energy and high intensity electron beam, which partly passes through the sample. The attenuation of the beam depends on the thickness and density of the sample, which enables the transmitted electrons to form a two-dimensional projection of the sample mass [28].

The size of silver particles supported on alumina was studied by TEM, using a JEOL JEM-1200 EX II instrument, in paper III and V.

4.2.7. Temperature programmed desorption and reduction

In temperature programmed reaction methods a chemical reaction is followed while the temperature increases linearly. If desorption processes are followed, they are normally preceded by adsorption of gas phase species at low temperature. For studies of reduction or oxidation characteristics, the sample is often exposed to H₂ or O₂, respectively, during the temperature ramp. These methods can provide valuable information on in particular surface sites.

NH₃-TPD – surface acidity. Surface acidity can be studied by temperature programmed desorption (TPD) of ammonia. Since the strongly basic ammonia molecule is relatively small (kinetic diameter 2.62 Å) and has a lone pair of electrons [113], it readily adsorbs onto acidic sites in the narrow pores of a catalyst support. After pre-treatment of the sample at high temperature it is saturated with ammonia at low temperature. When the temperature is increased at a constant rate in a flow of an inert gas, the desorbing ammonia is measured. The loosely bound ammonia desorbs at low temperature, while ammonia bound more strongly to the surface desorbs at higher temperature. Thus, the temperature at which a molecule desorbs reflects how strongly it is bound to the surface [28]. In addition, the area under the TPD curve is proportional to the amount of ammonia desorbing from different surface sites and thus the number of sites can be determined.

NO-TPD – adsorption/desorption characteristics. Temperature programmed desorption of NO (NO-TPD) provides information on adsorption sites for NO. The adsorption/desorption is dependent on the surroundings (temperature and gas composition), the surface coverage (first or second order desorption) and binding energy of the molecule to different adsorption sites. At low temperatures more gas can adsorb on the catalyst surface. During adsorption, one/some type(s) of surface sites may be occupied first, while the gas molecules bind to other types of sites at higher surface coverages [28]. Thus, the adsorption temperature and time, and gas concentration influences the subsequent desorption. The binding energy of the molecule to the catalyst surface is reflected in the temperature at which it desorbs. This enables discernment of different adsorption sites. [28].

H₂-TPR – reduction of silver by hydrogen. Temperature programmed reduction by hydrogen (H_2 -TPR) provides information on reduction of metallic catalysts [108]. The degree of reduction is followed over time, while the temperature increases linearly. The reduction of metal oxides by hydrogen begins by dissociative adsorption of hydrogen, where after the actual reduction is induced by atomic hydrogen [108]. Besides the dissociative adsorption, the reduction process involves diffusion of atomic hydrogen into the lattice, reaction with oxygen and removal of formed OH species [108]. Finally, the reduction of a metal oxide by H_2 normally results in formation of H_2O .

In this work surface acidity of monolith samples was investigated by temperature programmed desorption (TPD) of ammonia in a flow reactor in Paper I and VI. NO-TPD in excess oxygen with/without the presence of hydrogen was used to study differences between Ag/Al₂O₃ samples with different composition of silver species in paper V. The experiments were performed on monolith samples in a flow-reactor, analysing the outlet gas composition by gas phase FTIR. Furthermore, H_2 -TPR was performed for Ag/Al₂O₃ catalyst samples in Paper III and V. Powder samples were analysed in a differential scanning calorimeter, where the outlet gas composition was analysed by mass spectrometry (Hiden HPR-20 QUI).

4.2.8. DSC – adsorption of hydrogen

Differential scanning calorimetry (DSC) can provide information on chemical reactions and physical transitions by heat measurements. The change is measured for the difference in heat flow to the sample and a reference while they are subject to a controlled temperature program [114]. Adsorption is an exothermic process, while desorption is endothermic. In addition every chemical reaction is associated with a certain heat of reaction [114].

Differential scanning calorimetry (Setaram Sensys DSC) was used during the H_2 -TPR in paper III, to provide information on the adsorption of H_2 on the Ag/Al₂O₃ surface.

4.3. Catalytic performance

4.3.1. Flow reactor experiments

The catalytic performance with respect to lean NO_x reduction with methanol was studied using a continuous flow reactor, illustrated in Figure 4.2. The flow-reactor equipment consisted of three main parts; a gas inlet system, a reactor and a gas analyser. Feed gases (Ar, O₂, NO, NH₃, H₂) were introduced into the reactor via separate mass flow controllers (Bronkhorst Hi-Tech). Methanol was introduced to the reactor via a CEM-system (controlled evaporator mixer; Bronkhorst Hi-Tech); where the methanol and carrier gas (Ar) flows were controlled by mass flow controllers (Bronkhorst Hi-Tech). The monolith sample was placed in the reactor consisting of a horizontally mounted quartz-tube. Before and after the monolith sample an uncoated cordierite monolith was placed in order to

minimize temperature and flow gradients, as described by Wang-Hansen et al. [115]. The inlet gas temperature, used to control the reactor heating, was measured inside one of the channels in the centre of the uncoated monolith preceding the sample monolith. In addition the catalyst temperature was measured in the centre of the sample monolith. During the NO_x reduction reaction this temperature was always higher compared to the inlet temperature. The outlet gas composition was analysed by gas phase FTIR spectroscopy (MKS Instruments, MultiGas 2030) and mass spectrometry (Hiden HPR-20 QUI). The gas phase FTIR analyser was calibrated with known concentrations of the main reactants (methanol, NO) and products (NO₂, CO₂, CO, DME), while the mass spectrometer was calibrated with H₂.

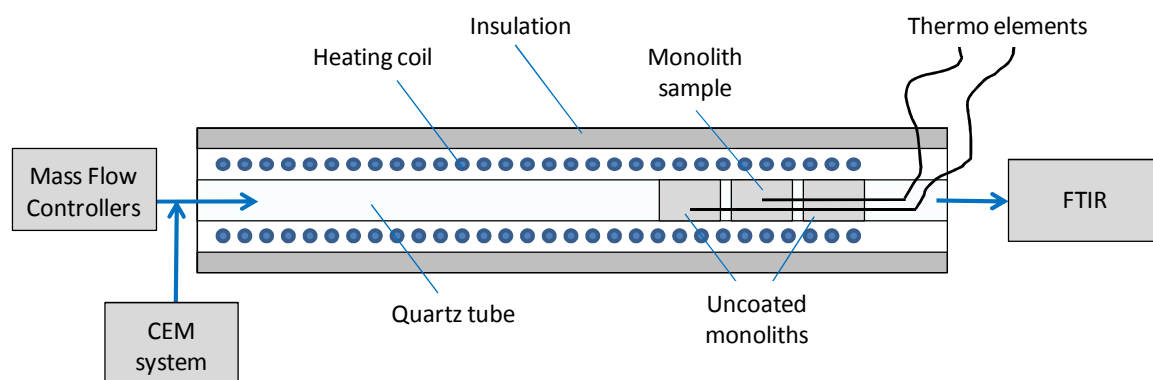


Figure 4.2. The flow reactor equipment.

4.3.2. Fourier Transform Infrared (FTIR) spectroscopy

Infrared spectroscopy is based on the ability of molecules to absorb or emit electromagnetic radiation in the infrared region. The absorption or emission of electromagnetic radiation results in a change in vibrational and/or rotational energy of a chemical bond, which is unique for the functional group or molecule. This allows for several species to be analysed simultaneously. An example is given in Figure 4.3, showing peaks of CO₂, CO, H₂O, NO, NO₂ and methanol. Unique absorption peaks are used for each species for identification and quantification. The absorption of infrared light occurs only when the vibrations result in a change in dipole moment. The intensity of the IR peak/band is proportional to the change in dipole moment. Polar groups like CO, NO and OH result in strong IR absorption, while covalent bonds (C-C, N=N) give weaker absorption. Symmetrical molecules like H₂, N₂ and O₂ cannot be detected by infrared spectroscopy, since they cannot form a dipole. In Fourier transform infrared (FTIR) spectroscopy interferences, caused by the movable mirror in the Michelson interferometer, are summed into an interferogram and Fourier transform is used to calculate a spectrum. The main advantages of a Fourier transform spectrometer, compared to an equivalent scanning monochromator, are an improved signal-to-noise ratio and a faster analysis.

FTIR spectroscopy can be used for analysis in gas or liquid phase or for solids. Diffuse reflectance infrared Fourier-transform spectroscopy (DRIFTS) provides information on species on the catalyst surface [108]. For bonds of gas phase species, vibrational and rotational transitions occur, while adsorbed species show only vibrational transitions. The unique peak(s) on the wave number scale associated with a molecule is influenced by the surrounding atoms, revealing for example information about the adsorption site. In diffuse reflectance mode the infrared radiation penetrates a short distance into the surface and the subsequently emerging diffuse components are measured. Molecules which adsorb on the surface or diffuse into the surface regions of the sample can thus be followed. With this technique thick or non-transparent powder samples can be analysed. It is, however, difficult to make quantitative analyses since it is difficult to estimate how deep into the sample the infrared radiation penetrates.

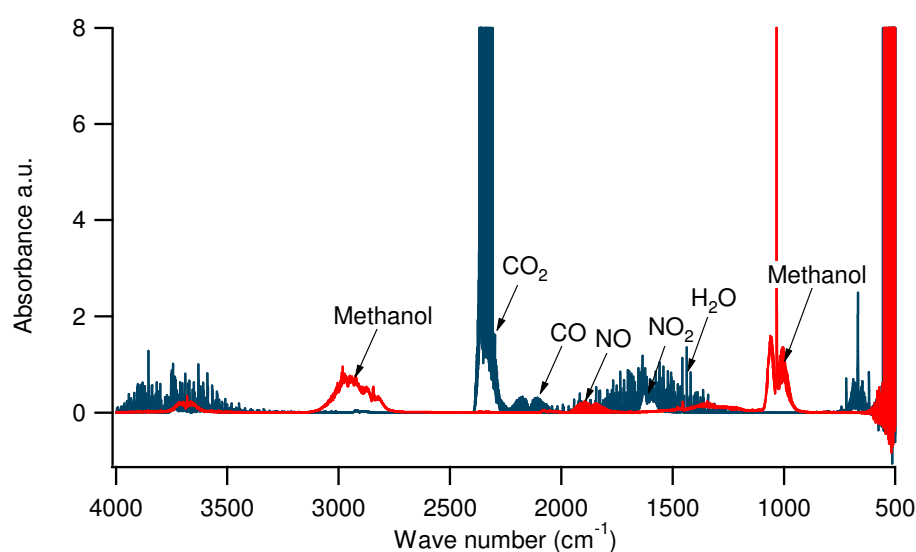


Figure 4.3. Example of FTIR spectra of gas phase species obtained during the present work.

In the present study a gas phase FTIR (MKS Instruments, MultiGas 2030) was used to analyse the gas phase species in the outlet of the flow reactor in all papers included in the thesis. Reported N_2 concentrations/yields are calculated from detected nitrogen species. DRIFT spectroscopy was used to follow surface species on Ag/Al_2O_3 and $\gamma-Al_2O_3$ during methanol oxidation, NO oxidation and methanol-SCR conditions in paper VI.

4.3.1. Mass spectrometry

In mass spectrometry ions are generated from the studied species. The ions are separated by their mass-to-charge ratio (m/z) and detected qualitatively and quantitatively [116]. The analysed species are identified based on their molecular mass or masses of fragments created during the ionization process.

Mass spectrometry (Hiden HPR-20 QUI) was used to analyse H_2 in the outlet of the flow-reactor in Paper IV and VI, and during the H_2 -TPR experiments in paper III and V.

5. Selective catalytic reduction with methanol

In the present work supported silver catalysts are evaluated for lean NO_x reduction with methanol. The aim is to increase the understanding of the catalytic processes relevant for achieving a high low-temperature activity. The catalyst preparation methods, characterization and flow-reactor equipment are described in section 4 above. The catalyst samples were studied in methanol-SCR and methanol oxidation conditions with respect to influence of the support material (section 5.1), the silver loading and composition of silver species (section 5.2), and the gas composition (section 5.3), including the observed formation of H₂ from methanol (section 5.4). During methanol-SCR conditions NO is reduced to N₂, N₂O and NH₃, and oxidized to NO₂. At the same time the reducing agent, methanol, is converted to mainly DME, formaldehyde, CO, CO₂, CH₄, H₂ and H₂O. The total conversion as well as the proportion of the reaction products depend on the catalyst composition, the inlet gas composition and the temperature.

5.1. *Influence of the support material*

The support material was characterized with respect to specific surface area and surface acidity, by NH₃-TPD, for alumina (Paper I and VI) and ZSM-5 based samples (Paper I). In addition the lean NO_x reduction with methanol was compared for alumina and ZSM-5 based samples (Paper I).

The specific surface area, measured according to the BET method, is higher for the ZSM-5 based samples (316 – 403 m²/g) compared to the Al₂O₃ based samples (176 - 220 m²/g). For the silver containing samples, the specific surface area is somewhat lower than for the samples without silver. The difference is likely owing to the silver covering some of the highly porous support material or caused by additional handling of the sample when the silver was introduced. A high surface area is thought to be beneficial for catalytic reactions in general. However, when comparing the silver containing samples in Figure 5.1a and b, the NO_x reduction is higher for the Ag/Al₂O₃ sample, which has a lower surface area, compared to the Ag-ZSM-5 sample. Here, obviously other aspects are more important. Furthermore, the NH₃-TPD profile for the alumina and ZSM-5 based samples in Figure 5.1c and d are remarkably different. The ZSM-5 based samples adsorb more NH₃, and NH₃ desorbs over a wider temperature range compared to over the alumina based samples. Moreover, the acidity is affected by the introduction of silver, likely by silver covering, or in other ways affecting, some of the acidic sites. This is also shown for Ag/Al₂O₃ samples studied by NH₃-TPD in Paper VI. Acidic sites are thought to be important for lean NO_x reduction with several reducing agents over both γ -Al₂O₃ and ZSM-5 based catalysts [117-120]. Accordingly, H-ZSM-5 shows both the highest acidity and gives the highest NO_x reduction amongst the ZSM-5 based samples in Figure 5.1. Similarly, the γ -Al₂O₃ sample shows the highest acidity and gives the highest NO_x reduction amongst the alumina based

samples. The NO_x reduction over the $\gamma\text{-Al}_2\text{O}_3$ sample, however, occurs at high temperature, while the $\text{Ag}/\text{Al}_2\text{O}_3$ sample is active at lower temperature. This advantage of the silver containing sample is obviously not connected to the number of acidic sites, since the desorption of NH_3 is lower for the $\text{Ag}/\text{Al}_2\text{O}_3$ sample in Figure 5.1c, compared to the $\gamma\text{-Al}_2\text{O}_3$ sample. Thus, even if alumina sites are involved in the lean NO_x reduction reactions over silver/alumina [119,120], they are not the most crucial factor influencing the NO_x reduction.

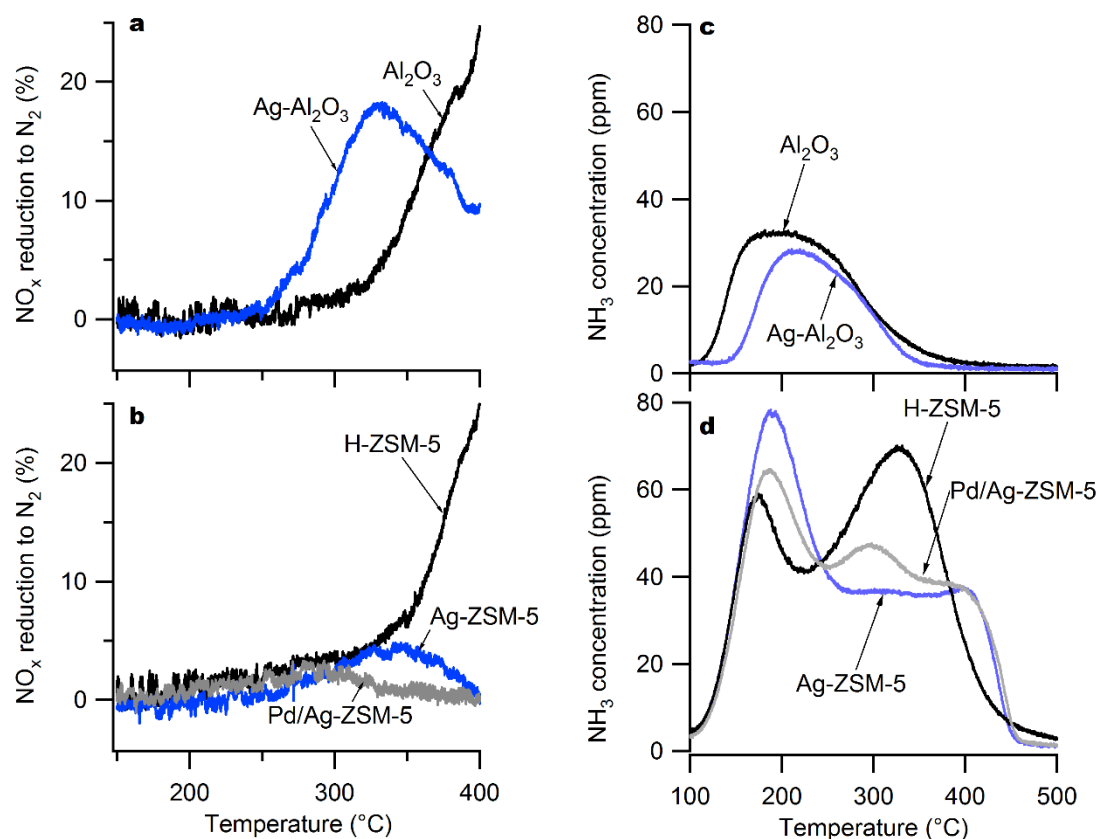


Figure 5.1. NO_x reduction to N_2 during cooling ramps over alumina based (a) and ZSM-5 based (b) samples. Inlet gas composition: methanol (850 ppm), NO (500 ppm), O_2 (10%) and Ar (bal.). NH_3 -TPD (in Ar, $10^\circ\text{C}/\text{min}$) for alumina based (c) and ZSM-5 based (d) samples, after exposure to 1000 ppm NH_3 until saturation at 100°C and flushing with Ar for 1 h.

Furthermore, the choice of support material influences the dispersion of silver. In Paper I, the UV-vis analysis indicates that the $\text{Ag}/\text{Al}_2\text{O}_3$ and $\text{Ag}/\text{ZSM-5}$ samples both contain highly dispersed silver species, i.e. mainly ions and small clusters. The silver loading for the samples is, however, different, i.e. ca 2 wt% Ag for the $\text{Ag}/\text{Al}_2\text{O}_3$ sample and ca 5 wt% Ag for the $\text{Ag}/\text{ZSM-5}$ sample. A higher silver loading normally results in a lower dispersion of silver (and is further discussed in section 5.2 below), i.e. when comparing silver species on the same support material for samples prepared by the same method. Here, however, the

dispersion of silver seems to be similar for the Ag/Al₂O₃ and the Ag-ZSM-5 samples (in Paper I), despite the differences in silver loading. This might be related to differences in the support material, like the specific surface area, the pore size or the atomic structure of the material. However, also the preparation method influences the dispersion of silver and is further discussed in section 5.2 below. Finally, it should also be noted that comparison of the UV-vis spectra in Paper I is difficult, especially at high wavelengths, owing to insufficient pre-treatment of the samples. The samples should have been analysed directly after calcination like in Paper V.

To summarize, the investigations regarding the support material, it can be concluded that a high specific surface area or a high acidity is not crucial for achieving a high NO_x reduction at low temperature over supported silver catalysts when using methanol as reducing agent. Other factors are more important in this case, like the dispersion of silver, which is discussed below.

5.2. *Influence of silver species*

In order to investigate the influence of the silver loading on the lean NO_x reduction with methanol (Paper II-IV), Ag/Al₂O₃ catalysts were prepared according to a previously described sol-gel method [41]. The influence of the composition of silver species was studied using another set of Ag/Al₂O₃ samples with comparable silver loading, prepared utilizing different preparation methods (Paper V and VI). The aim was to investigate the influence of the composition of silver species, separately from the influence of the silver loading. The preparation methods used were physical mixing, microemulsion, sol-gel and acid leaching. The silver species supported on alumina were characterized by UV-vis spectroscopy, TEM and H₂-TPR, and their influence on the desorption of pre-adsorbed NO was studied by NO-TPD in the presence of O₂ and H₂ (Paper I, III, IV and V). The catalytic performance of the samples was studied in flow-reactor experiments during methanol-SCR and methanol oxidation conditions (Paper I, II, V and VI).

Small oxidized silver clusters (Ag_n^{δ+}) or ions (Ag⁺) are thought to be important for the formation of N₂ during the lean NO_x reduction over Ag/Al₂O₃ [33]. Metallic silver particles, on the other hand, are known to cause combustion of the reducing agent, but might also play a role in the NO_x reduction mechanism, possibly by promoting oxidation reactions, like oxidation of NO to NO₂ [46]. Thus, the composition of silver species is important for the lean NO_x reduction over supported silver catalysts, and motivates the study of the influence of silver species in the present work. The choice of preparation method has been found to influence the dispersion of silver on supported catalysts. For example, the sol-gel method used for preparation of Ag/Al₂O₃ samples in the present work is reported to result in high amounts of silver ions and small oxidized silver clusters [41,121] and Paper V, while Ag/Al₂O₃ prepared by conventional impregnation, contains more metallic silver nanoparticles [41]. Moreover, as mentioned in section 5.1 above, the silver loading is known to influence the dispersion. High silver loadings was found by Bethke and Kung

[33] to result in metallic silver nanoparticles, while silver in lower amounts is reported to be present as small oxidized silver species [33]. Thus, both the Ag loading and the preparation method influence the dispersion of silver in the catalyst, and consequently also the NO_x reduction performance.

TEM analysis. The size of silver particles was investigated by TEM in Paper III for Ag/Al₂O₃ samples of different silver loading (1 – 10 wt% Ag, sol-gel). Silver nanoparticles of mainly ca 10 – 15 nm are observed for the 10 and 4 wt% Ag samples. No obvious difference between the particle sizes for these two samples of different silver loading is found. For the 1 wt% Ag sample, on the other hand, no particles are clearly visible in the TEM images. If silver nanoparticles are present for the 1 wt% Ag sample, they are too small (< ca 5 nm) to be seen in the resolution of the TEM instrument used. Thus, clearly, a difference in silver loading between 1 and 4 wt% Ag results in a difference in the size of the silver particles on the Ag/Al₂O₃ surface.

Furthermore, the size of silver particles was investigated by TEM in Paper V for Ag/Al₂O₃ samples prepared by different methods. The TEM analysis reveal large silver nanoparticles (> 20 nm) in the samples prepared by physically mixing γ -Al₂O₃ and Ag₂O. These samples were prepared with the intention to create a low dispersion of silver, i.e. the mixing was carried out in a mortar for only a short period of time, before the calcination at 600 °C. Such large particles are not observed for the samples prepared by other methods. A common silver particle size in the 4% Ag samples prepared by microemulsion and the sol-gel method is ca 10 – 15 nm, according to the TEM analysis. The intention with choosing a microemulsion method was to create nanoparticles of a defined size. This should be possible since the size of a microemulsion droplet to a far extent controls the size of the metal particle created inside. The size of the silver particles created in the microemulsion in the present work, however, seems to be similar to those created when using the sol-gel method, which was expected to give a higher dispersion of silver. The number of silver nanoparticles is, on the other hand, not studied for the two samples and might thus be different. For the LE4 sample prepared by leaching a sol-gel sample in nitric acid, however, slightly smaller silver particles are observed (ca 5 nm) than for the other 4% Ag samples, when studying several TEM images including those in Paper V. The intention with choosing the leaching method was to prepare samples with a high dispersion of silver, higher than what can be achieved by the sol-gel method alone. For the 1% Ag samples prepared by the sol-gel method and acid leaching, respectively, no nanoparticles are visible in the performed TEM analysis, unlike for the other 1% Ag samples (prepared by the microemulsion method and physical mixing). The resolution of the TEM instrument is, however, not high enough to enable an exact analysis of the silver nanoparticles. Nevertheless, an indication of an order of particle size can be discerned by studying the TEM images. The size order for the samples prepared by different methods appears to be as follows, from small to large particles: LE < SG < ME < MX.

UV-vis spectroscopy. Further information regarding the composition of silver species is obtained from characterization by UV-vis spectroscopy. The spectra of recently calcined Ag/Al₂O₃ samples are presented in Figure 5.2, after subtraction of the spectrum of a γ -Al₂O₃ sample prepared by the same method as each silver containing sample. The assignment of the absorbance in different wavelength regions to different types of silver species is described in Paper I, IV and V. Figure 5.2a shows the influence of the silver loading on the UV-vis spectra for Ag/Al₂O₃ samples prepared by the sol-gel method. The spectra shows that all samples contain silver ions (peak at ca 220 nm), small silver clusters (Ag_n^{m+}, ca 250 – 380 nm), and silver nanoparticles (> ca 400 nm). The absorbance, corresponding to all types of silver species, is higher when the silver loading is higher. It can, however, be realized from Figure 5.2a that the proportion of the different silver species is different for the compared samples, which is confirmed by comparing peak areas after deconvolution. For example the increase in the number of silver clusters appears to be higher than the increase in the number of silver ions, when comparing the samples with 1 and 4 wt% Ag. Another example is that the difference in the number of silver ions appears to be much smaller than the difference in the number of larger Ag species (clusters and particles), when comparing the samples with 4 and 10 wt% Ag. Thus, a higher silver loading implies a higher proportion of large silver species.

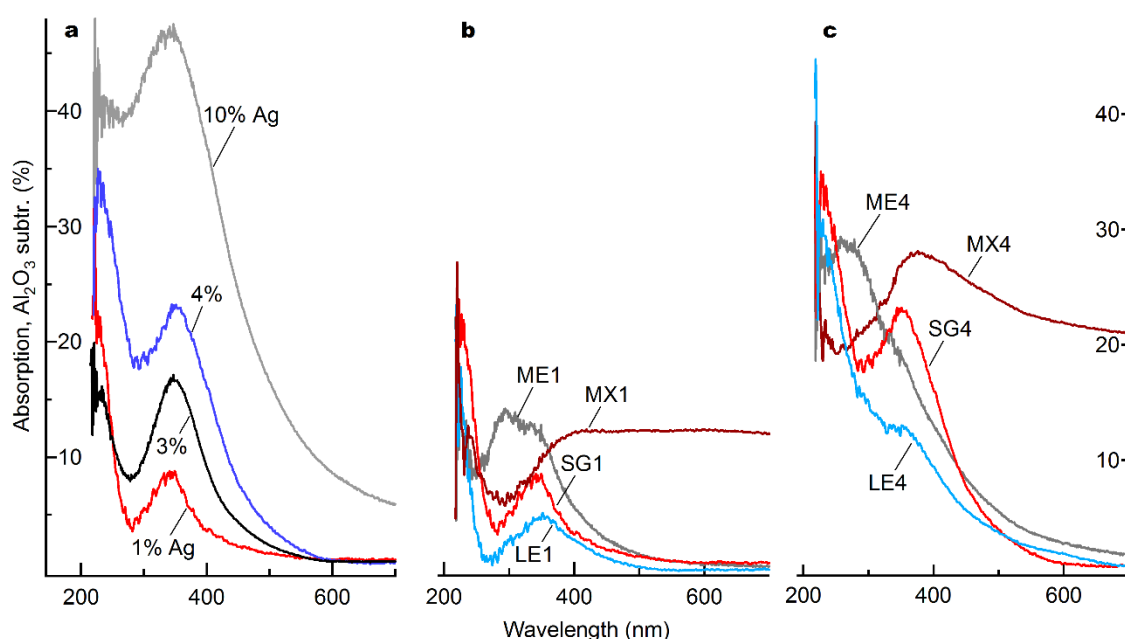


Figure 5.2. UV-vis spectra of Ag/Al₂O₃ samples after subtraction of the spectrum for a γ -Al₂O₃ sample prepared by the same method. The spectra were taken after calcination in air (600 °C, 6h). a) Samples with different silver loading, prepared by the sol-gel method. b) Samples with ca 1.4 wt% Ag and c) samples with ca 4 wt% Ag, prepared by physical mixing (MX), microemulsion (ME), the sol-gel method (SG) and acid leaching (LE).

UV-vis spectra for Ag/Al₂O₃ samples prepared by different methods are presented in Figure 5.2b (ca 1 wt% Ag) and Figure 5.2c (ca 4 wt% Ag). The spectra are considerably different for the compared samples. The small differences in the measured silver content of the samples (up to ca +/- 15 %) cannot explain the differences between the UV-vis spectra. According to the TEM analysis the physically mixed samples contain larger silver nanoparticles compared to the samples prepared by other methods. This is supported by the high absorbance above 400 nm for the MX1 and MX4 samples in Figure 5.2b and c. Contributing factors to the high absorbance in a wide wavelength range above 400 nm are likely a high number of silver nanoparticles and a broad size distribution. In addition the shape of the particles could influence the UV-vis spectrum. The presence of high amounts of Ag₂O seems unlikely, based on the comparison with spectra for an uncalcined mixture of alumina and Ag₂O, and alumina and metallic silver powder, respectively, described in Paper IV. Furthermore, the samples prepared according to the microemulsion method were expected to contain a high number of nanoparticles. According to Figure 5.2c and d, however, the absorbance above 400 nm for the ME1 and ME4 samples is considerably lower compared to the physically mixed samples (MX1 and MX4). An explanation could be that the ME1 and ME4 samples contain no large (> ca 20 nm) nanoparticles, like the MX1 and MX4 samples, according to the TEM analysis. Obviously also the number of nanoparticles, which was not studied in detail, influences the absorbance. In addition to nanoparticles the ME1 and ME4 samples contain a high number of small silver clusters (Figure 5.2b and c), which appear to be different from those in the other samples, i.e. the absorbance peaks are noted at slightly different wavelengths. Possible differences regarding the clusters could be variations in the number of silver atoms, the arrangement of the atoms of the cluster and the oxidation state. Moreover, the highest number of silver ions (Ag⁺) is found for the samples prepared by the sol-gel method and acid leaching (Figure 5.2b and c). The number of silver ions is slightly lower for the leached samples compared to the sol-gel samples. Also the number of silver clusters and nanoparticles is lower for the leached samples compared to the sol-gel samples, and there the difference is larger than for the ions. Especially the LE4 sample contains significantly less silver clusters and particles, compared to the SG4 sample. Thus, the proportion of silver ions appears to be higher for the leached samples compared to the sol-gel samples. In other words, mainly larger silver species are removed by leaching, but the silver ions are also affected.

Reduction/oxidation properties. The reduction of silver species was studied by H₂-TPR for sol-gel Ag/Al₂O₃ samples with different silver loading in Paper III, and for Ag/Al₂O₃ samples prepared by different methods in Paper V. In addition reduced and oxidized Ag/Al₂O₃ samples were compared by UV-vis spectroscopy in Paper IV.

During SCR conditions the silver species on Ag/Al₂O₃ are exposed to the reducing agent and any added H₂, as well as high concentrations of oxygen. Changes in the gas composition and the temperature cause changes with respect to the supported silver species (oxidation state and size), which in turn influences the NO_x reduction performance of the catalyst. Figure 5.3 illustrates the influence of different gas mixtures on the supported silver

species in Ag/Al₂O₃. Exposure to a flow of NO and O₂ in argon at 260 °C does not make a significant change to the UV-vis spectrum (shown for a 5 wt% Ag sample in Figure 5.3a) or the colour of the samples (Figure 5.3b, lower panel), compared to the recently calcined samples. When methanol is included in the flow (at 260 °C), however, the UV-vis spectrum and the colour of the samples containing 3 – 10 wt% Ag changes. Moreover, after exposure to a flow of H₂ (in argon) at 200 °C the change in the spectrum and the colour is more extensive, and now also noticeable for the 1 wt% Ag sample. These experiments illustrate the importance of the gas composition for the oxidation/reduction of silver species, where the influence of methanol is especially interesting in the context of methanol-SCR which is in focus in the present work.

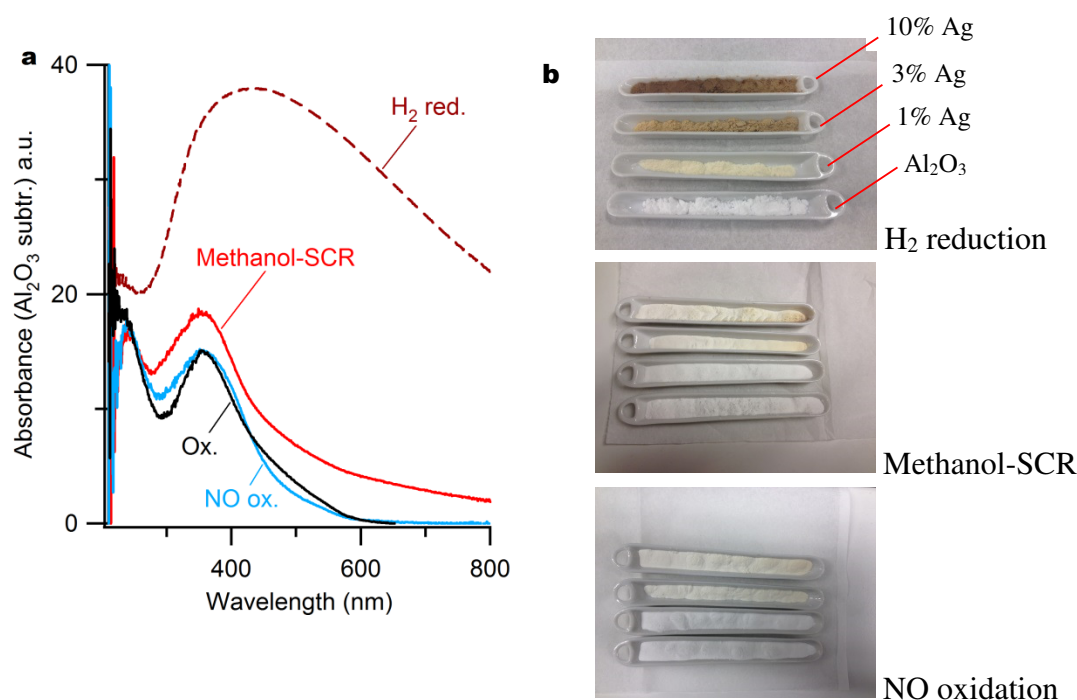
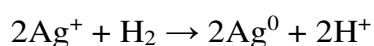
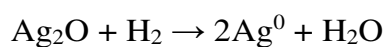


Figure 5.3. a) UV-vis spectra of a Ag/Al₂O₃ sample (5 wt% Ag, sol-gel) after subtraction of the spectrum for a γ -Al₂O₃ sample exposed to the same pre-treatment as the silver containing sample. b) Ag/Al₂O₃ samples with different silver loading (10, 3, 1 and 0 wt% Ag, sol-gel), after different pre-treatment. The samples were exposed to calcination in air (600 °C, 6h), NO and O₂ at 260 °C, a methanol-SCR gas mixture at 260 °C and H₂ at 200 °C, respectively. Gas concentrations (when used): NO 500 ppm, methanol 5000 ppm, O₂ 10%, H₂ 2000 ppm and Ar (bal.).

Further information regarding the reduction/oxidation of silver species is obtained by H₂-TPR. During H₂-TPR hydrogen is thought to reduce silver, for example by the following reactions [59]:



Measurements of the consumption of H₂ should, thus, give an indication of how many silver atoms are reduced. In addition the above reaction schemes show that observation of water in the outlet of the reactor could be an indication of what type of silver species are reacting with H₂. Care has however to be taken when interpreting the data, since the silver species can be partly or completely reduced (to metallic silver). In addition, silver particles could be reduced only on the surface or throughout the whole particle, i.e. different types of adsorbed oxygen species could react with H₂ [122]. However, comparing samples using the same experimental method should give an indication of differences regarding the reducibility of the silver species. Furthermore, large silver species/particles are assumed to be loosely bound to the support, while small silver species are more strongly bound. The more strongly bound (small) species are thought to be more difficult to reduce and thus require a higher temperature for reduction to occur [33]. Thus, the H₂ consumption at low temperatures should originate in reduction of large silver species. It should though be noted that large supported silver species, i.e. nanoparticles, usually are described as metallic, rather than as a silver oxide. Metallic particles can obviously not be further reduced and would thus not induce any H₂ consumption. Reduction of supported silver and Ag₂O was investigated by Richter et al. [59], who noted no H₂ consumption for a calcined mixture of Ag₂O and alumina, where Ag₂O presumably had decomposed into metallic silver during the calcination at high temperature (500 °C, 5% O₂). For an uncalcined mixture, on the other hand, H₂ consumption was observed. In this context it can be understood that many reports suggest that somewhat smaller silver species, i.e. small oxidized silver clusters (designated Ag₂O or Ag_n^{m+}) are reduced at low temperature during H₂-TPR ([33,47,59] and references therein).

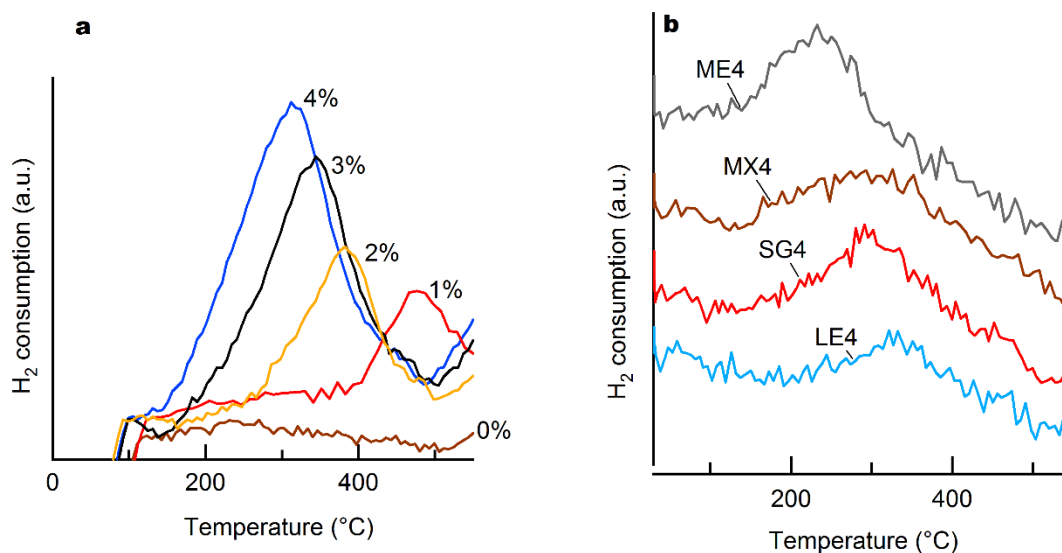


Figure 5.4. H₂ consumption during heating (10 °C/min) in a flow of 2000 ppm H₂ in Ar, over Ag/Al₂O₃ samples a) with different silver loading, prepared by the sol-gel method and b) samples with similar silver loading, prepared by different methods, i.e. physical mixing (MX), microemulsion (ME), sol-gel (SG) and acid leaching (LE). The curves in b are offset for readability.

Figure 5.4a shows the H₂ consumption over Ag/Al₂O₃ samples after pre-treatment in a flow of oxygen (10% O₂ in Ar) at high temperature (550 °C). After cooling to 30 °C (in 10% O₂), and flushing with argon, the sample is exposed to a flow of 2000 ppm H₂ during heating. Already at low temperature (30 °C) a small consumption of H₂ occurs over the silver containing samples, in accordance with Sayah et al. [123]. At higher temperature further H₂ consumption occurs. For the γ -Al₂O₃ sample no consumption of H₂ is observed above ca 100 °C, while it for the silver containing samples increases with the silver loading. In addition, the consumption of H₂, in Figure 5.4a, occurs at higher temperature for the samples containing less silver, which implies that the low-loaded samples contain smaller and/or more strongly bound silver species, in accordance with previous studies [47,59]. Furthermore, the fraction of silver reduced during the whole H₂-TPR experiment is calculated and presented in Paper III. For the samples containing 1 – 3 wt% silver the fraction of silver which is reduced increases with increasing silver loading, while the fraction of silver reduced for the 4 wt% Ag sample is approximately the same as for the 3 wt% Ag sample. Thus, the proportion of the type(s) of silver species which is/are reduced during the H₂-TPR for the 3% Ag sample is higher compared to the 1 % Ag, but similar as for the 4 % Ag sample. Based on the TEM and UV-vis results above it is concluded that the proportion of nanoparticles is increasing with increasing silver loading, which could indicate that nanoparticles are reduced during the H₂-TPR. This, on the other hand, implies that the nanoparticles would be in an oxidized form. If the nanoparticles consist of Ag₂O (or other oxygen containing silver species) water is expected to be formed. Some water is observed in the outlet of the reactor during the first part of the heating (< 400 °C). However, no clear connection to the silver loading is found. In addition, as discussed above, the nanoparticles are in most reports thought to be in metallic form already after the calcination, which is also assumed based on the UV-vis analysis above. Hence, silver nanoparticles are not a likely candidate to be reduced during the H₂-TPR. Furthermore, comparisons with the UV-vis analysis does not provide a clear answer to if the silver species reduced during the H₂-TPR are silver clusters or ions, but assuming that larger silver species can be reduced at lower temperature, small oxidized silver clusters are the most likely candidate. Whether the clusters are partly or completely reduced cannot be determined based on the performed experiments. At high temperatures (> 500 °C) in Figure 5.4a an increase in the H₂ consumption is seen. This could be explained by reduction of smaller or more strongly bound silver species, i.e. silver ions or more strongly bound small clusters. It can, however, not be ruled out that this H₂ consumption occurs on the alumina support since a small increase in H₂ consumption is seen also for alumina at these temperatures (Figure 5.4a).

Figure 5.4b shows the H₂ consumption over Ag/Al₂O₃ samples of comparable silver loading, which are prepared by different methods. During these experiments the signal to noise ratio for the mass spectrometer was not optimal, but the temperature for the H₂ consumption peaks can nevertheless be compared. Assuming that the H₂ consumption in the studied temperature range originates in reduction of small oxidized silver clusters, as discussed in connection to Figure 5.4a above, it can be concluded that the stability against reduction for the silver clusters in the compared samples increases in the following order:

ME4 < MX4 < SG4 < LE4. Thus, the clusters in the compared samples appear to have slightly different oxidation/reduction properties, which could be explained by size or structural differences of the clusters or that the clusters are bound to different sites in the support structure, which results in different bonding strengths.

NO-TPD. Desorption of NO_x was studied in Paper V for Ag/Al₂O₃ and γ-Al₂O₃ samples prepared by different methods. The complete experiment, including adsorption and desorption was carried out in oxygen excess, and was repeated with 2000 ppm H₂ present in the flow (Ar balance). NO adsorbs in the presence of excess oxygen in different forms, mainly as different types of nitrates and nitrites on alumina as well as on silver [20,63,124]. The surface NO_x(ads) species play an important role in the lean NO_x reduction over Ag/Al₂O₃ and are influenced by H₂. They have been extensively studied, for example using NO_x-TPD experiments [63,125-129]. In the present work the desorption of NO_x in oxygen excess is compared for samples with different composition of silver species. Knowing that H₂ has a large impact on the adsorption/desorption of NO_x(ads) species on Ag/Al₂O₃, experiments with and without H₂ in the feed were compared. The aim was to gain information about the influence of different types of silver species on the desorption of NO_x. The experiments were performed in oxygen excess in order to mimic SCR conditions.

Figure 5.5a shows examples of desorption profiles for the experiments without H₂ in the feed, which are similar to those obtained by Chaieb et al. [128]. The results show only small differences for the desorption of NO_x in the absence of H₂, regardless of the silver loading or composition of silver species in the samples (Figure 5.5a). When H₂ is included in the feed the desorption profiles are, on the other hand, significantly different for the compared samples, as illustrated for the physically mixed samples in Figure 5.5b. In the presence of H₂ the silver has an extensive impact on the desorption of NO_x. In the literature, adsorbed NO_x species have been identified to have different roles in the lean NO_x reduction process. Some are taking part in the reduction reactions, while others are blocking surface sites (hindering adsorption of other species). Yet another category of surface NO_x species are described as spectator species, which are not taking part in the NO_x reduction reactions [63,124]. In Paper V H₂ is found to remove surface NO_x(ads) species at low temperature. This in accordance with the suggestion by Azis et al. [125] that H₂ helps to remove possibly inhibiting surface NO_x(ads) species at low temperature. Furthermore, when comparing the results from the experiments including H₂ in the feed, some desorption peaks were found to appear at approximately the same temperature for all samples, while one in particular shifted in temperature, as illustrated in Figure 5.5c. Since the composition of silver species is known to influence the temperature at which the NO_x reduction occurs, the desorption peak appearing at different temperatures is especially interesting to study. This peak is more likely to have an influence on the lean NO_x reduction reactions and can possibly be related to the so called H₂ effect, while the desorption peaks not shifting in temperature are more likely to be spectator species. Figure 5.5c shows that the shift in temperature for the marked NO desorption peak roughly follows the change in size of the supported silver species, which is described based on TEM and UV-vis analyses above.

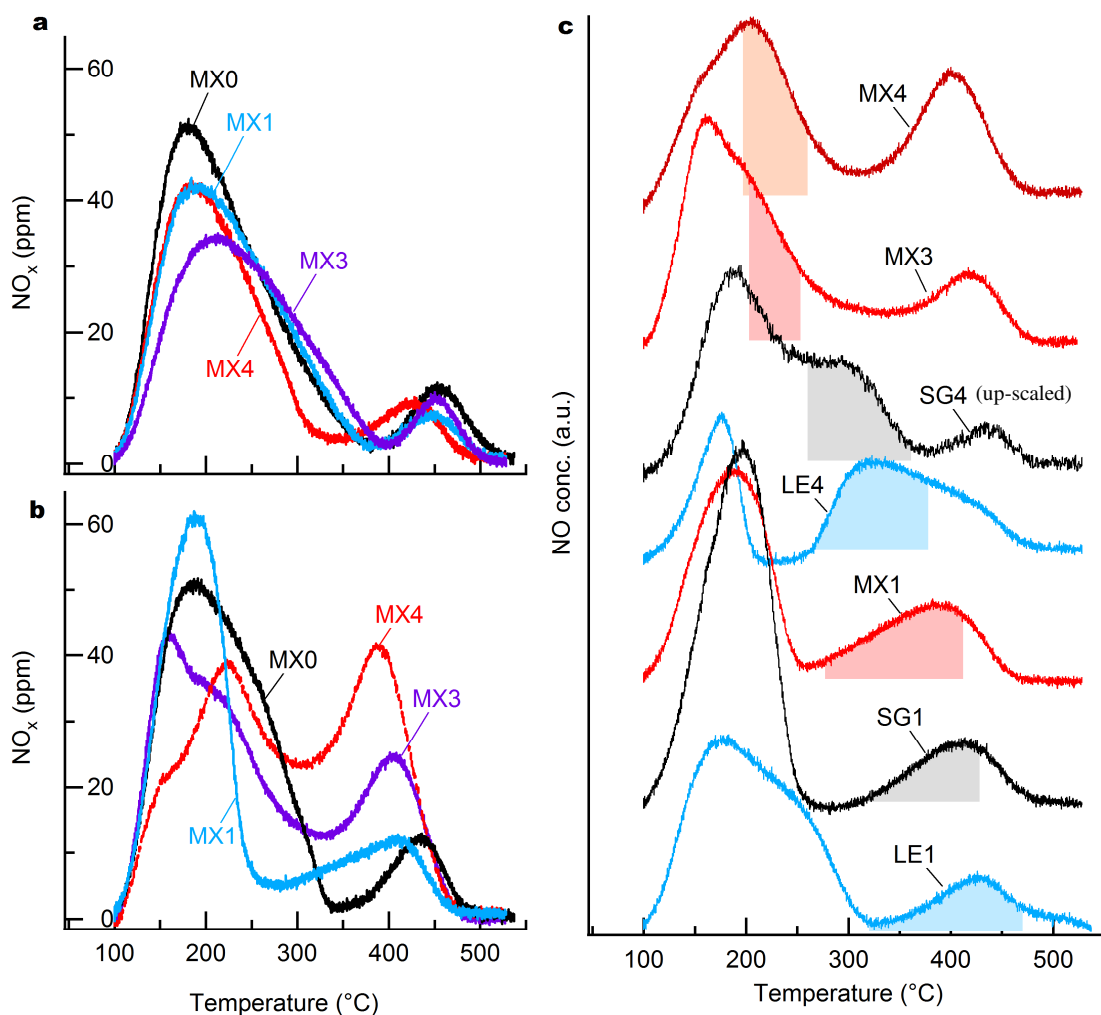


Figure 5.5. Desorption of NO_x during temperature increase after adsorption of NO (500 ppm) in a flow of 10% O_2 in argon a) in the absence of H_2 b) and c) in the presence of 2000 ppm H_2 . The samples are prepared by physical mixing (MX), the sol-gel method (SG) and acid leaching (LE). The number in the sample name indicates the approximate wt% of Ag. Coloured areas in c) mark a desorption peak appearing at different temperature. The curves in c) are offset and the curve for SG4 (where problems with the gas flows occurred) is up-scaled for readability.

Methanol-SCR. The main gas phase species formed during methanol-SCR experiments over $\text{Ag}/\text{Al}_2\text{O}_3$ are presented in Figure 5.6. Figure 5.6a shows the results for a set of $\text{Ag}/\text{Al}_2\text{O}_3$ samples with different silver loading (0 – 4 wt%) prepared according to the sol-gel method (Paper II). A higher silver loading clearly promotes catalytic activity at low temperature in addition to oxidation reactions (more NO_2 and CO_2 is formed) and formation of N_2O , while the formation of DME, and CO and N_2 at high temperature is suppressed. Furthermore, a higher silver loading, within the weight-% range studied in Figure 5.6a, enhances the formation of N_2 at low temperature. Even higher silver loadings (ca 5 - 12 wt% Ag), however, result in a low conversion of NO , with a shift towards higher N_2O

formation on the expense of the N_2 formation (not shown). Furthermore, Figure 5.6b illustrates the formation of gas phase species during lean NO_x reduction with methanol over two sets of Ag/Al_2O_3 samples with comparable silver loading. The target silver loading for the two sets of samples prepared according to different methods were 1.4 and 4.1 wt% Ag, respectively. The actual Ag loading (presented in Paper V), however, differs somewhat from the target, but the differences between the samples are concluded to be of minor importance, compared to the differences in the composition of silver species. Moreover, since the silver loading of the MX4 sample is rather high (4.5 wt% Ag), an additional sample with 3.0 wt% Ag (MX3) was prepared by physical mixing, in order to further distinguish between the effect of silver loading and the composition of silver species.

Figure 5.6b confirms the findings from Figure 5.6a that the samples with higher silver loading (ca 4 wt% Ag) are active at lower temperature compared to the other samples (with ca 1 wt% Ag). However, for the different samples with ca 1 wt% Ag, in Figure 5.6b, the temperature at which the lean NO_x reduction takes place is significantly different and does not follow the small differences in silver loading. The maximum N_2 formation occurs at different temperatures for the compared samples, in the following order from low to high temperature: MX1 \ll ME1 < SG1 \ll LE1. When this temperature order is compared with the results from the TEM and UV-vis analyses, a similar order is found for a range of silver species. Based on these comparisons, we in Paper V, suggest that the lean NO_x reduction at low temperature (Figure 5.6b) is promoted by silver clusters and/or small silver particles (< ca 20 nm). No such relation is found for the single silver ions or larger silver particles (> 20 nm), which are suggested not to influence the temperature for NO_x reduction.

Furthermore, Figure 5.6b shows that the selectivity to N_2 is in general lower for the samples containing more silver (ca 4 wt% Ag), compared to those with lower silver loading (ca 1 wt% Ag). Probably the small silver species predominantly present in low-loaded samples promote a high selectivity to N_2 , while the higher amounts of large silver species present in the high-loaded samples result in a higher formation of N_2O . This is supported by a high formation of N_2O over the SG4 and MX4 samples, concluded to contain a high number of silver nanoparticles according to the UV-vis and TEM analysis. Over the LE4 sample, on the other hand more N_2 is formed, at the same time as the UV-vis analysis indicate more small silver species (i.e. ions and small clusters), compared to SG4 and MX4. Thus silver nanoparticles can be concluded to promote formation of N_2O , while smaller silver species are important for the N_2 formation. Furthermore, the selectivity to N_2 for the samples MX1 and LE4 is remarkably similar, even if their silver loading is significantly different (1.6 and 3.8 wt% Ag). An explanation can most likely be found in the composition of silver species, i.e. a high proportion of small silver species (ions and/or clusters) in combination with low amounts of somewhat larger silver species. The exact size or nature of these larger silver species cannot be determined based on the performed experiments.

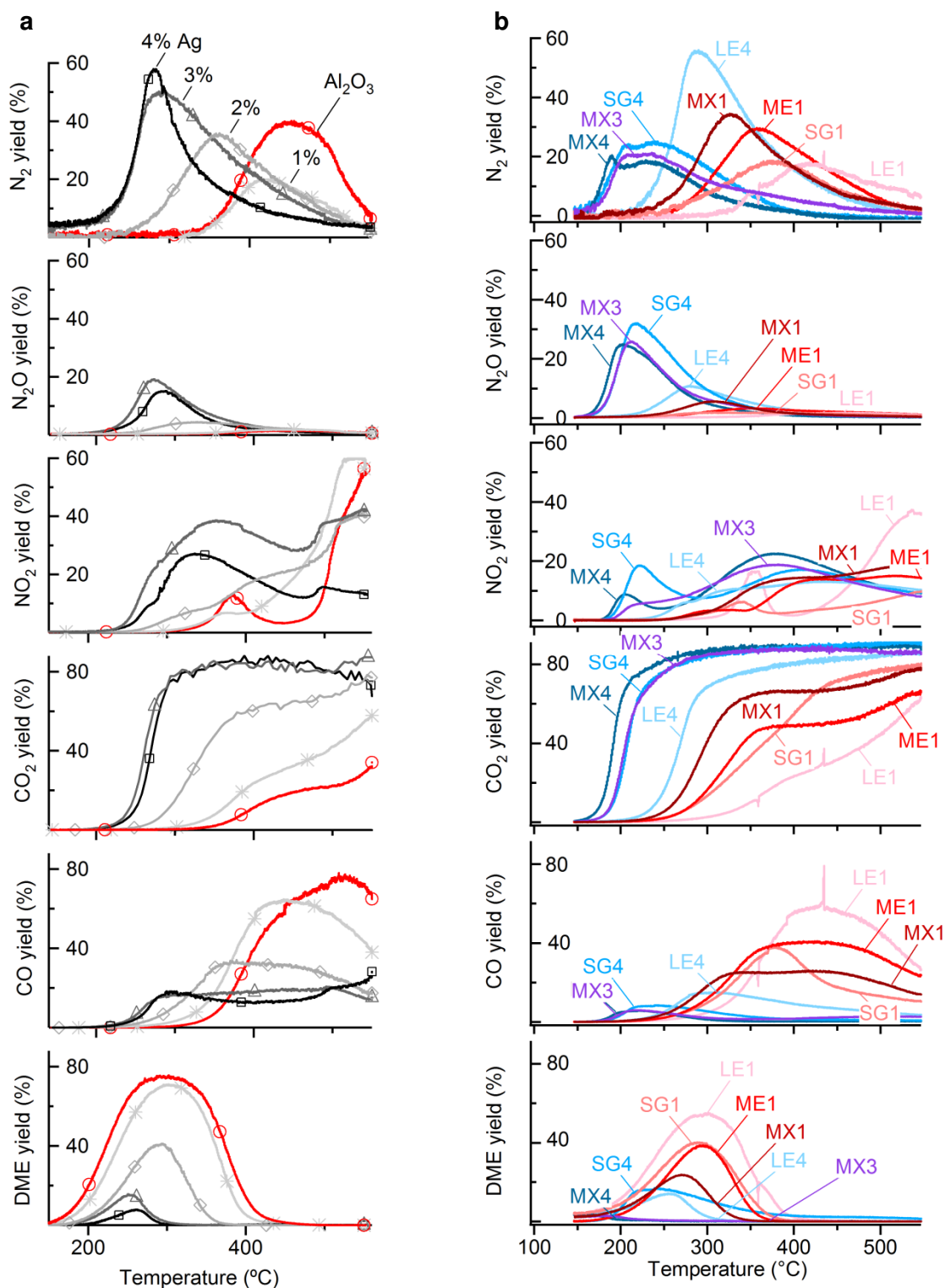


Figure 5.6. Lean NO_x reduction with methanol during cooling ramps over Ag/Al₂O₃: a) samples prepared according to the sol-gel method (wt% of Ag indicated in the figure), and b) samples prepared according to different methods, i.e. physical mixing (MX), microemulsion (ME), sol-gel (SG) and acid leaching (LE). The number in the sample name indicates the approximate wt% of Ag. Inlet gas composition: 1700 ppm CH₃OH, 500 ppm NO, 10% O₂ and Ar (bal.).

One size range of nanoparticles could though be excluded, i.e. the nanoparticles larger than ca 20 nm observed by TEM for the physically mixed samples, suggested above to result in the remarkably high absorbance > 400 nm in the UV-vis spectra for MX1 and MX4 in Figure 5.2b and c. The NO_x reduction results in Figure 5.6b, however, do not show such large differences for the physically mixed samples compared to the others. Thus, the large nanoparticles (> ca 20 nm) are suggested not to influence the selectivity to N₂.

Moreover, in Figure 5.6, there seems to be a critical point around ca 4 wt% Ag, above which the NO_x reduction performance deteriorates, similar to the optimum silver surface density proposed by Chaieb et al. [128]. For the samples in Figure 5.6 with a silver loading close to 4 wt% Ag the formation of N₂ and N₂O is significantly different. Here, apparently, small differences in the properties of the catalytic material have a large impact on the catalytic performance. It can be realized, when comparing the results for the LE4, MX3 and MX4 samples in Figure 5.6b, that the composition of silver species is more important in this respect than silver loading. The N₂ formation is similar for the MX3 and MX4 samples, while it is significantly higher for the LE4 sample. The silver loading for LE4 (3.8 wt% Ag), on the other hand, lies between those for MX3 (3.0 wt% Ag) and MX4 (4.5 wt% Ag). Thus, it can be concluded that the selectivity to N₂ is influenced by the composition of silver species.

To summarize, the influence of silver species on the lean NO_x reduction with methanol over Ag/Al₂O₃, it can be concluded that both the silver loading and the composition of silver species are important. Mainly it is the number of silver species of certain types that matters. Often, however, a combination of different types of silver species can explain a certain behaviour, like the similar selectivity to N₂ for the LE4 and MX1 samples in Figure 5.6b. Furthermore, we show that Ag/Al₂O₃ samples with similar silver loading but significantly different composition of silver species can be realized by utilizing different preparation methods. The samples show differences in the desorption of NO in the presence of O₂ (excess) and H₂, and an NO desorption peak related to the differences in the composition of silver species is observed. The samples also show different reduction characteristics when reduced with H₂, and reduction of silver during methanol-SCR reaction conditions is indicated by UV-vis analyses.

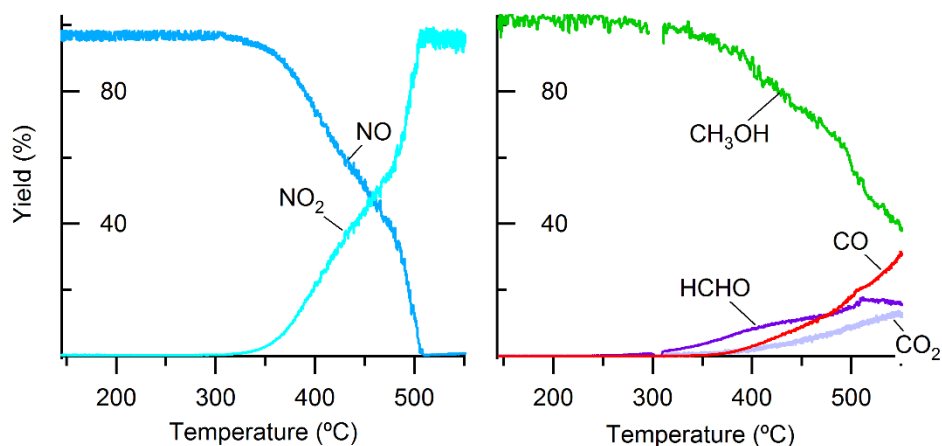


Figure 5.7. Lean NO_x reduction with methanol during cooling ramps for an empty reactor tube. Inlet gas composition: 1,700 ppm CH_3OH , 500 ppm NO , 10% O_2 and Ar (bal.).

5.3. Influence of gas composition

The influence of the C/N ratio on the lean NO_x reduction with methanol over $\text{Ag}/\text{Al}_2\text{O}_3$ was investigated by changing the inlet concentration of methanol in Paper I and by changing the inlet concentration of NO in Paper II. The influence of NO on the conversion of methanol was studied in Paper II and V. In addition the influence of O_2 on the methanol conversion was investigated in Paper VI.

First, it should be noted that the composition of the methanol containing gas mixture fed into the reactor changes before it reaches the catalyst sample. As illustrated in Figure 5.7 for a methanol-SCR gas mixture flowing through an empty reactor tube, at temperatures above ca 300 °C conversion of methanol occurs, with formation of mainly formaldehyde, CO and CO_2 . In the same temperature range NO conversion to NO_2 occurs, with complete conversion above 500 °C. The oxidation of NO to NO_2 is likely induced by radical reactions initiated by methanol and O_2 , similar to those described for DME and O_2 by Tamm et al. [130]. The inlet gas composition obviously influences the catalytic performance. For example, the high NO_2 concentration at high temperatures likely enhances the lean NO_x reduction, while the CO_2 formation at high temperature should give a lower catalytic activity than what could be expected for the same concentration of methanol in the feed.

Higher inlet concentration of methanol during methanol-SCR experiments over $\text{Ag}/\text{Al}_2\text{O}_3$ in Paper I, resulted in enhanced NO_x reduction at 350 °C. Owing to the positive results changes of the C/N ratio was further investigated in Paper II. This time we chose to alter the inlet concentration of NO , mainly owing to easier control of the gaseous NO , compared to the liquid methanol. The experiments were carried out in steady-state conditions at 250 - 350 °C and the NO_x reduction is shown in Figure 5.8. The results show that by increasing the C/N molar ratio to a certain extent (at least to ca 7) the formation of N_2 can be enhanced.

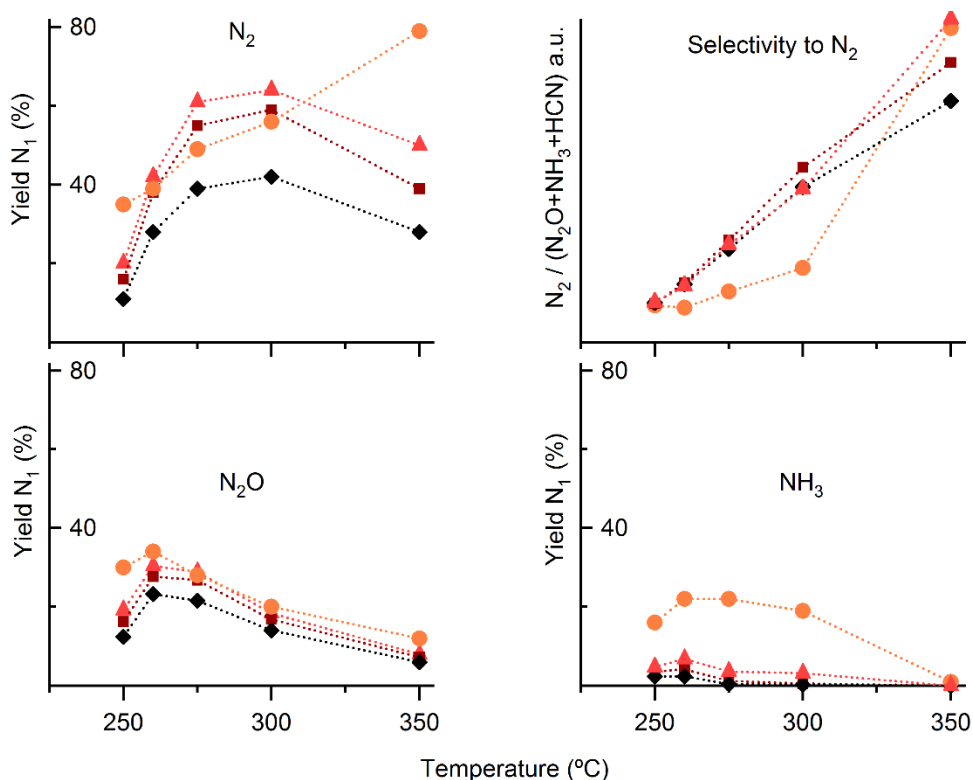


Figure 5.8. Reduction of NO during methanol-SCR experiments over Ag/Al₂O₃ (3 wt% Ag) at steady-state conditions. Inlet gas: 1,700 ppm methanol, 10% O₂, 500 ppm NO (black rhombus), 333 ppm NO (brown square), 250 ppm NO (red triangle) and 100 ppm NO (orange circle).

At the same time also the formation of N₂O increases and for high C/N ratios (C/N=17) significant formation of NH₃ occurs (> 20 % yield at 270 °C). Figure 5.8, shows however that the selectivity to N₂ does not significantly change at low temperature when the inlet NO concentration is lowered, except for the lowest NO concentration (C/N=17). At high temperature the selectivity to N₂, in fact, increases with increasing C/N ratio. Higher C/N ratios also result in lower NO₂ formation, while the conversion of methanol is not much influenced, in accordance with the results in Paper I where the concentration of methanol was altered. Finally, it can be concluded that a moderate increase of the C/N molar ratio is beneficial for the lean NO_x reduction with methanol over Ag/Al₂O₃. It should though be kept in mind that increasing the feed of the reducing agent is costly and might result in higher amounts of unwanted carbon species (CO, formaldehyde, DME), which might have to be cleaned up after the SCR catalyst.

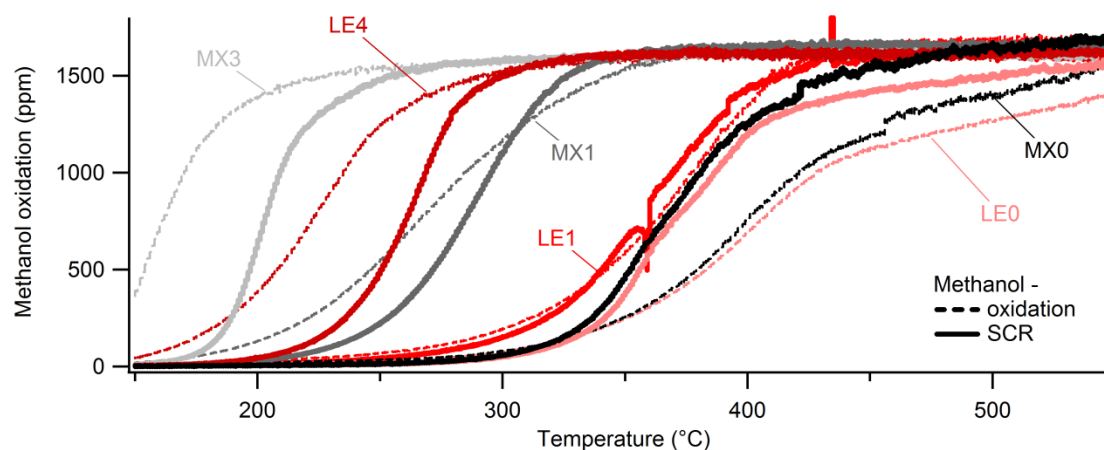


Figure 5.9. Methanol oxidation over $\text{Ag}/\text{Al}_2\text{O}_3$, in the presence and absence of NO. Experimental conditions: cooling ramps in 10% O_2 , 1,700 ppm CH_3OH , 0 (dashed lines) or 500 ppm (solid lines) NO, Ar (bal.). The samples were prepared by acid leaching (LE, brown/red) and physical mixing (MX, grey/black). The number in the sample name indicates the approximate wt% of Ag.

Methanol oxidation is compared for experiments with and without NO in the feed, in Paper VI. Figure 5.9 shows, as an example, the methanol oxidation over the samples prepared by acid leaching and physical mixing. The oxidation of methanol occurs at lower temperature in the absence (compared to the presence) of NO for the samples with high silver loading (3 – 4 % Ag), while the opposite can be observed for the $\gamma\text{-Al}_2\text{O}_3$ samples. The promotional effect of NO on the oxidation of methanol over the $\gamma\text{-Al}_2\text{O}_3$ samples, is explained by oxidation of NO to NO_2 at high temperature before the gas mixture reaches the catalyst sample (Figure 5.7). Moreover, the methanol oxidation, for the MX3 and LE4 samples in Figure 5.9, occurs at higher temperature in the presence of NO, compared to in its absence. One possible explanation is that NO and methanol are competing for the same adsorption sites on silver, and that the adsorbed NO species hinder the adsorption (and thus the oxidation) of methanol. For the MX3 and LE4 samples the methanol oxidation occurs at lower temperature compared to the other samples, containing less silver. The difference compared to the other samples can be explained by the fact that NO adsorbs more easily on the catalyst surface at low temperatures. Thus, if more NO is adsorbed on the active oxidation sites, it could more efficiently hinder the adsorption of methanol. This can explain why methanol oxidation for MX3 and LE4 occurs at lower temperature in the absence of NO (compared to in its presence), while the difference between the experiments with and without NO is small for the samples containing less silver (MX1 and LE1).

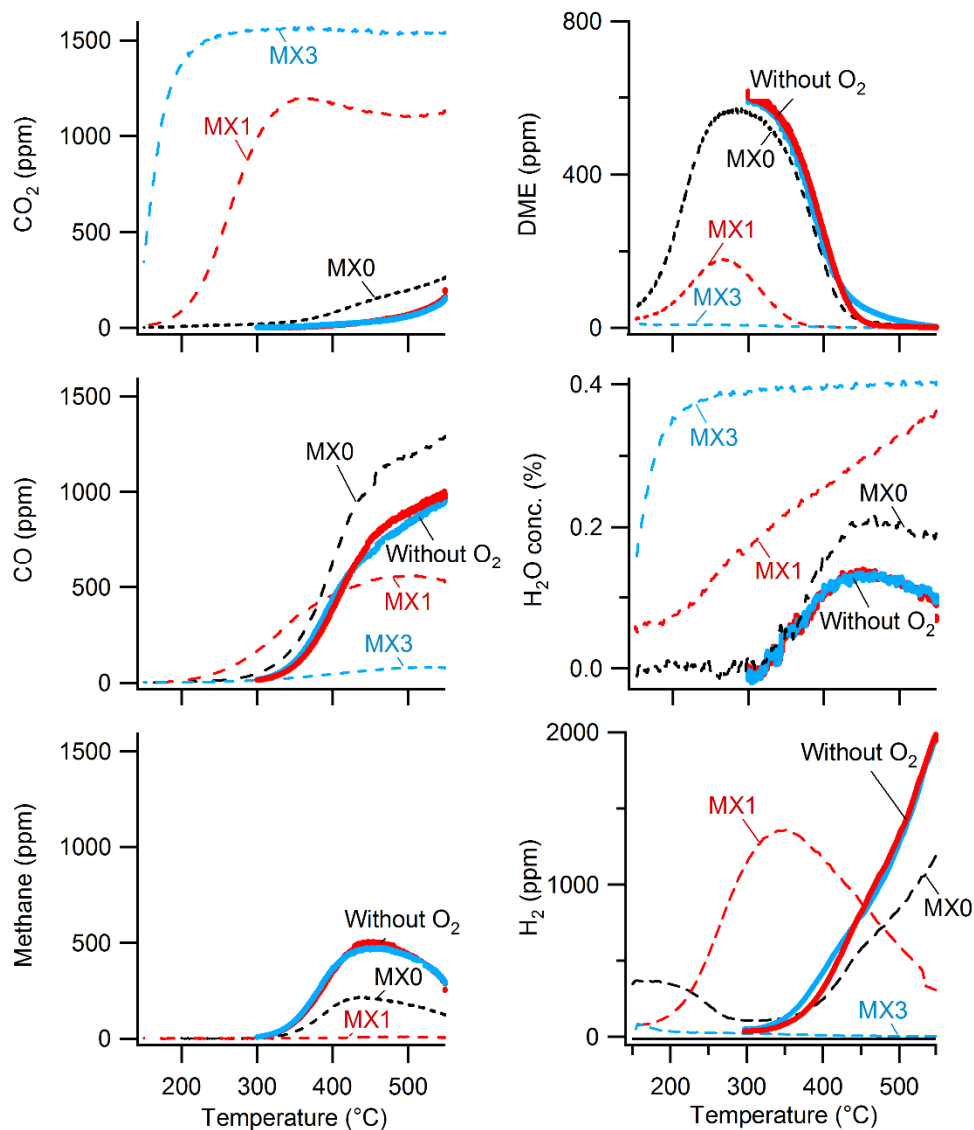


Figure 5.10. Methanol oxidation in the presence and absence of O_2 . Cooling ramps in 1,700 ppm CH_3OH , 0 (solid lines) or 10% (dashed lines) O_2 , Ar (bal.). The Ag/Al_2O_3 samples prepared by physical mixing contain ca 3 (MX3, blue), 1 (MX1, red) and 0 (MX0, black) wt% Ag.

The role of oxygen for the conversion of methanol over Ag/Al_2O_3 was investigated in flow-reactor experiments, in Paper VI, with and without O_2 in the feed. Figure 5.10 shows the outlet concentrations of the main gas phase species formed over Ag/Al_2O_3 and $\gamma-Al_2O_3$ samples prepared by physical mixing. Only the silver containing samples were tested without O_2 in the feed and Figure 5.10 shows large differences between the experiments performed in the absence and presence of O_2 . Interestingly, the results in Figure 5.10 for the experiments without O_2 in the feed are similar to each other, regardless of the difference in silver loading between the samples (MX3 and MX1). In the absence of O_2 the silver loading is obviously not important. In fact, the results for Ag/Al_2O_3 in the absence of O_2

shows similarities with the results for γ -Al₂O₃ with O₂ in the feed. Thus, it is assumed in Paper VI that the supported silver species in the absence of O₂ in the feed do not catalyse the reactions, but that the reactions rather occur on the alumina support. Apparently methanol is adsorbed and converted on alumina also in the absence of O₂. Figure 5.10 shows a slightly higher degree of oxidation of the carbon species over the γ -Al₂O₃ sample in the presence of O₂, compared to the experiments without O₂. This indicates that O₂ participates in the methanol oxidation reactions over γ -Al₂O₃. Furthermore, in the absence of O₂ it can be assumed that the supported silver species are in a more reduced state than when O₂ is present. It is likely that no reactions with methanol occur on reduced silver, but only when adsorbed oxygen atoms are present i.e. when the silver is in a more oxidized state. This is in accordance with Stegelmann and Stoltze [131], who found that ethylene could adsorb on both reduced and oxidized silver, but reactions occurred only on oxidized silver.

To summarize, the influence of the gas composition on the lean NO_x reduction with methanol over Ag/Al₂O₃, it can be concluded that both the NO reduction as well as the methanol oxidation are affected. The reduction of NO can be enhanced by a moderate increase of the C/N molar ratio, which does not deteriorate the selectivity to N₂. Furthermore, the oxidation of methanol over Ag/Al₂O₃ is influenced by the presence of O₂ and NO, in combination with the supported silver species. The C/N molar ratio, however, does not have a large impact on the composition of conversion products formed from methanol.

5.4. Formation and influence of hydrogen

The addition of H₂ to the HC-SCR feed is known to enhance the lean NO_x reduction over Ag/Al₂O₃. In Paper I, II and III the influence of addition of H₂ was investigated for methanol-SCR over Ag/Al₂O₃. The effect, however, turned out to be relatively small compared to what has been shown for non-oxygenated hydrocarbons, in accordance with Johnson et al. [76]. During the experiments presented in Paper IV, on the other hand, H₂ formation from methanol was observed during lean NO_x reduction over Ag/Al₂O₃. These findings led to further investigation of parameters influencing the H₂ formation, like the silver loading (Paper IV), the composition of silver species (Paper VI) and the gas composition (Paper IV and VI). Furthermore, the route for formation of H₂ from methanol was discussed in Paper VI.

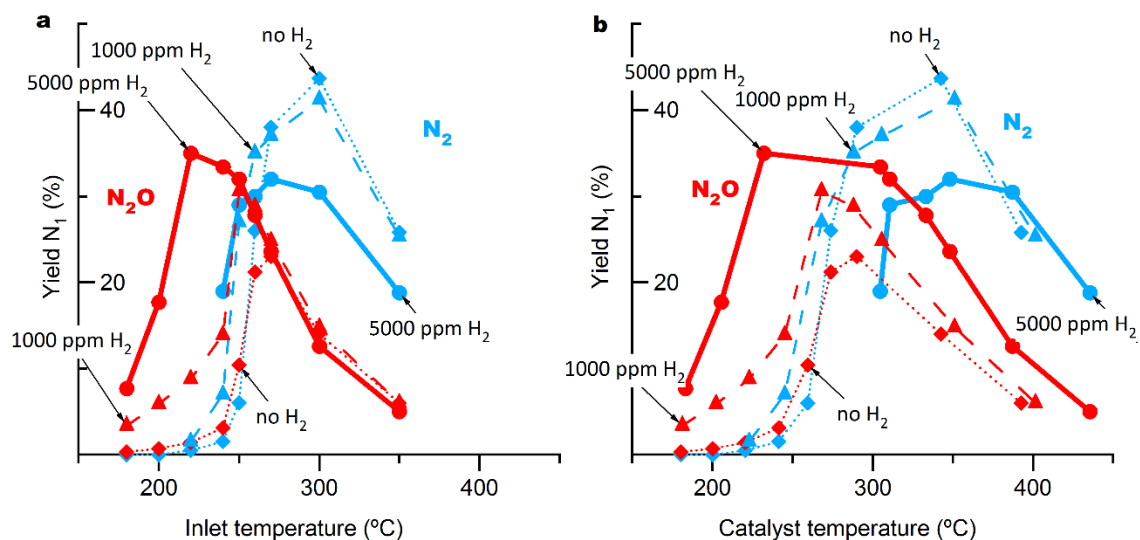


Figure 5.11. Formation of N_2 and N_2O over Ag/Al_2O_3 (3 wt% Ag) during methanol-SCR conditions at steady-state (steps 30 min), plotted vs. a) the inlet temperature and b) the temperature in the centre of the sample monolith. Inlet gas mixture: 1700 ppm methanol, 10 % O_2 , 500 ppm NO and 0 – 5000 ppm H_2 .

The influence of H_2 on the lean NO_x reduction with methanol over Ag/Al_2O_3 (3 wt% Ag , sol-gel) is tested using different concentrations of H_2 . Figure 5.11a shows that NO is mainly reduced to N_2 at high temperatures ($> ca\ 240\ ^\circ C$), while more N_2O is formed at low temperatures. When H_2 is included in the feed the formation of N_2 starts at slightly lower temperature, which is also shown for 4 and 2 wt% Ag samples in Paper III. However, also the formation of N_2O at low temperature is promoted by the addition of H_2 . In fact, at high H_2 concentrations (5000 ppm) N_2O is the main reaction product from NO_x reduction below $ca\ 240\ ^\circ C$ (Figure 5.11a). At higher temperatures ($ca\ 260 - 280\ ^\circ C$) the addition of H_2 suppresses the formation of N_2 . This could be explained by a more extensive formation of H_2O (especially when 5000 ppm H_2 is added), since experiments with H_2O included in the feed resulted in lower NO_x reduction (not shown). At even higher temperatures the decrease in N_2 formation upon H_2 addition can be explained by a temperature increase. When H_2 is included in the feed the temperature in the catalyst sample increases, owing to exothermic reactions. This can be realized when comparing the results plotted against the temperature measured at two different locations, i.e. $ca\ 1\ cm$ upstream of the sample (inlet temperature, Figure 5.11a) and in the centre of the sample monolith (catalyst temperature, Figure 5.11b). In Figure 5.11b the N_2 yield at high temperature (at 300 - 350 $^\circ C$ inlet temperature) coincides for the different H_2 concentrations, which shows that the apparently lower N_2 formation in Figure 5.11a can be explained by the temperature increase. Comparing the N_2O formation at high temperature in Figure 5.11a and b, on the other hand, indicates a different behaviour than for the N_2 formation. The N_2O formation for the compared experiments coincides at high temperature in Figure 5.11a, but not in Figure 5.11b, unlike

for the N_2 formation. This indicates differences in the formation route of the two species (N_2 and N_2O), like formation over different active sites and/or via different reaction mechanisms. This is in line with the suggestions in section 5.2 above, where N_2O formation is found to be promoted by silver nanoparticles, while smaller silver species contribute to the formation of N_2 . However, owing to the high N_2O formation the benefit of adding H_2 to the feed can be questioned for methanol-SCR applications.

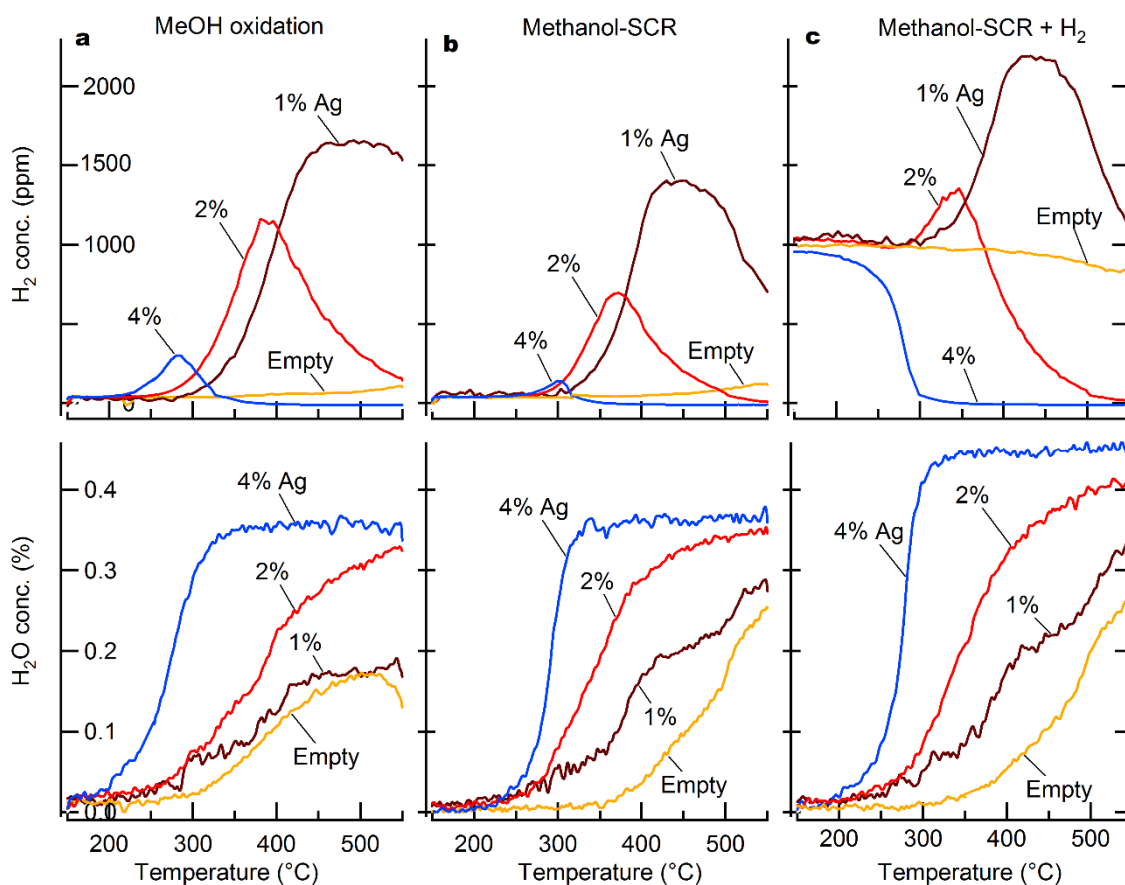


Figure 5.12. Outlet concentrations of H_2 and H_2O during cooling ramps over Ag/Al_2O_3 (4, 2, 1 wt% Ag) and in an empty reactor tube (i.e. no catalyst sample). Inlet gas mixture: a) O_2 and methanol, b) O_2 , methanol and NO, c) O_2 , methanol, NO and H_2 . Inlet gas concentrations (when used): 10% O_2 , 1,700 ppm CH_3OH , 500 ppm NO, 1000 ppm H_2 and Ar (bal.)

The low promotional effect of the H_2 addition in Figure 5.11 can to some extent be understood when considering that H_2 is formed during the methanol-SCR reactions. Figure 5.12 shows the formation of H_2 and H_2O from methanol in different gas compositions over Ag/Al_2O_3 samples with 1 – 4 wt% Ag. Results from experiments performed with an empty reactor tube are included for comparison. Figure 5.12 shows that more H_2 is present in the outlet of the flow-reactor for samples with lower silver loading, while more H_2O is formed

over the samples containing more silver. Possibly, H₂ or molecular hydrogen is formed also over the samples with higher silver loading, where it could influence the catalytic reactions before it is oxidized to H₂O. Furthermore, comparisons of Figure 5.12a and b shows that less H₂ is present in the outlet when NO is included in the feed. A possible explanation is that H₂ formed from methanol has been consumed during the catalytic reactions, resulting in the accompanying higher formation of H₂O. Figure 5.12c illustrates the high oxidation ability of Ag/Al₂O₃ with high silver loading, where all co-fed H₂ is oxidized to H₂O at high temperature (> ca 300 °C for the 4% Ag sample). Most likely it is the silver nanoparticles present in high numbers in the samples with high silver loading, which enhance the oxidation of H₂. Moreover, the influence of the composition of silver species for the H₂ formation during methanol oxidation experiments was investigated in Paper VI. The temperature for the apparent H₂ formation for the compared samples can to some extent be related to the composition of silver species, where large silver species or particles seem to promote H₂ formation at low temperature, but also oxidation of H₂ to H₂O at high temperature. The concentration of the formed H₂ can, however, not be compared for the investigated samples, owing to experimental difficulties.

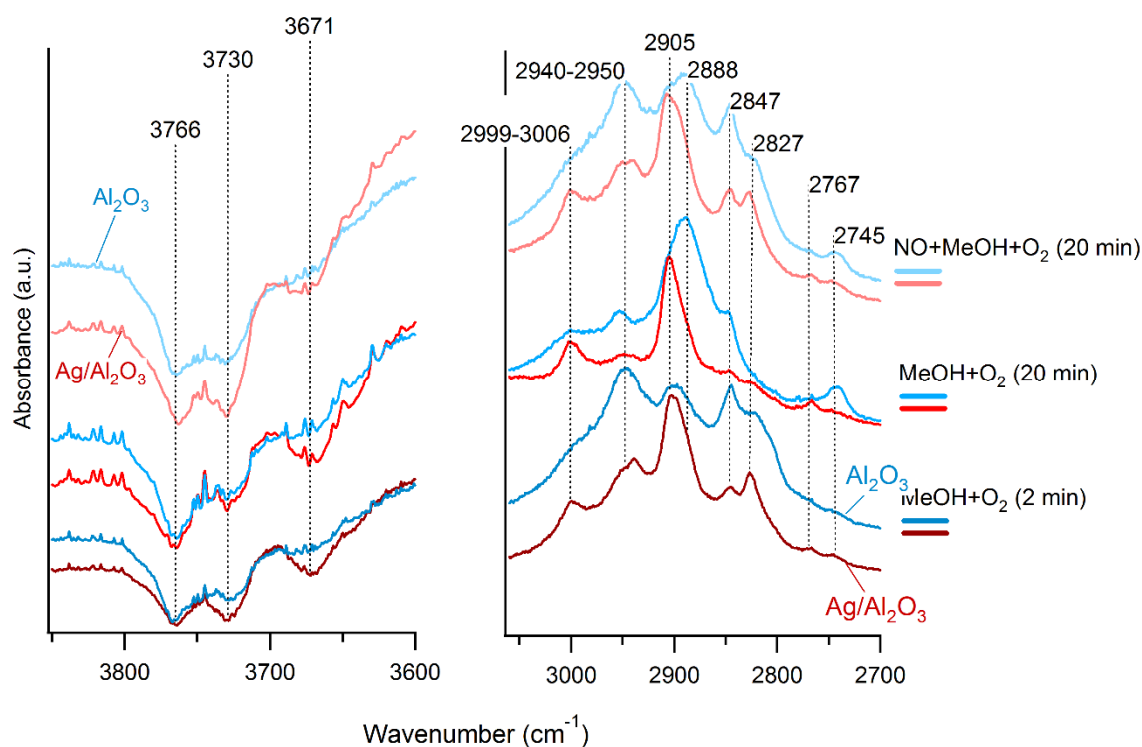


Figure 5.13. DRIFT spectra of Ag/Al₂O₃ and γ -Al₂O₃ samples at 260 °C during methanol oxidation and methanol-SCR conditions. Inlet flow: O₂ (10%), methanol (4000 ppm), NO (0 or 500 ppm), and argon (bal.). The time mentioned in the figure indicates time passed since the gas composition was changed. The spectra are offset for readability.

Ag/Al₂O₃ and γ -Al₂O₃ samples were studied during methanol oxidation and methanol-SCR conditions using DRIFT spectroscopy, in Paper VI. The pre-oxidized catalyst samples were exposed to a flow of methanol and O₂ for 20 min before NO was introduced. Figure 5.13 shows the changes for the hydroxyl groups on the catalyst surface in the region 3850 – 3600 cm⁻¹ and the development of adsorbed carbon containing species in the region 3100 – 2700 cm⁻¹. The assignments of the peaks are reported in Paper VI. When methanol is adsorbed negative absorption bands appear in the OH-region in Figure 5.13 at 3766, 3730 and 3671 cm⁻¹, and the negative peaks grow deeper when NO is introduced. This indicates that methanol and NO adsorb on the same type of OH-sites on the alumina support on both Ag/Al₂O₃ and γ -Al₂O₃, with some differences in the amounts adsorbed on the different sites of the compared samples. Moreover, Figure 5.13 shows that formate (-O-CH-O-) species are more prominent on the surface of the Ag/Al₂O₃ sample, while more methoxy groups (-O-CH₃) are formed on the γ -Al₂O₃ surface. The presence of formates is reflected in the higher formation of CO₂ and CO over Ag/Al₂O₃ at the present temperature (260 °C), compared to over γ -Al₂O₃ (Figure 5.6). The higher formation of methoxy groups on the γ -Al₂O₃ sample, on the other hand, results in a higher DME formation (at 260 °C) compared to the silver containing sample (Figure 5.6). The observed formates and methoxy groups on the catalyst surface are obviously formed from the conversion of methanol [98,132,133]. When methanol loses its hydrogen atoms different adsorbed or gas phase carbon containing species are formed. This conversion of methanol also leads to the formation of H₂ and H₂O. For example, when methanol is adsorbed on the catalyst surface as methoxy groups (CH₃-O-), hydrogen atoms are released and either adsorbed on the surface or reacting with oxygen to form H₂O. If the methoxy groups react with each other or with methanol to form DME (CH₃-O-CH₃), one oxygen atom or an OH- group is left over. The oxygen or OH-group can bind to the surface or react with hydrogen atoms to form H₂O. Furthermore, the methoxy groups can lose hydrogen atoms and form dioxy-methylene (CH₂-O-O-) or formates (CH-O-O-). These can in turn leave the surface as formaldehyde (HCHO), and CO or CO₂. At the same time adsorbed species containing H and/or O atoms, and gas phase H₂ and H₂O can be formed. Moreover, Figure 5.10 shows that the H₂O and H₂ formation occur in the same temperature interval as the methanol conversion. Interestingly, however, no H₂ or H₂O is accompanying the DME formation at 300 °C (and below) for the γ -Al₂O₃ sample and for the experiments without O₂ in the feed (Figure 5.10). Thus, this could be an indication of that the hydrogen atoms released, when methanol is adsorbed as methoxy groups, bind to the catalyst surface. Formation of H₂ was also seen for γ -Al₂O₃ samples and during the experiments without O₂ over Ag/Al₂O₃ at high temperature (Figure 5.10). Thus, it seems likely that the alumina support is involved in the H₂ formation over Ag/Al₂O₃ and that the role of silver (in the presence of O₂) is to shift the reactions to lower temperature. The exact mechanism is, however, not revealed by the performed experiments.

To summarize the studies of H₂ in connection to methanol-SCR over Ag/Al₂O₃, it can be concluded that H₂ is formed from methanol and further addition of H₂ to the feed does not provide obvious benefits. Hydrogen atoms are released during the conversion of methanol. Possibly, the high NO_x reduction at low temperature for oxygenated reducing agents is more associated with the adsorbed hydrogen atoms, than with the subsequently formed gaseous H₂. This could explain why a high low-temperature activity is seen also for Ag/Al₂O₃ with fairly high silver loading, where not so much H₂ is present in the outlet of the reactor during methanol-SCR conditions, but more H₂O. The adsorbed hydrogen atoms might have been present also there and influenced the NO_x reduction reactions before oxidation to H₂O occurs. Furthermore, the effect of H₂ for methanol-SCR over Ag/Al₂O₃ is discussed in the present work. Reduction of silver (Figure 5.3) is observed when Ag/Al₂O₃ is exposed to H₂ and a methanol-SCR gas mixture, respectively. Another effect of H₂, which is described in the present work is its influence on the desorption of NO_x (Figure 5.5), and in Paper IV and VI indications of removal of nitrates and adsorbed CN species by H₂ are discussed.

6. Concluding remarks

Methanol, which is considered a promising renewable fuel, is in the present work evaluated as reducing agent for NO_x under lean conditions over supported silver catalysts. The aim is to gain increased understanding of factors influencing catalytic activity and selectivity, especially at low temperature. The role of the supported silver is studied, together with the influence of the support material and the gas composition, including the formation of hydrogen.

During the initial methanol-SCR studies, $\text{Ag}/\text{Al}_2\text{O}_3$ shows a higher NO_x reduction at low temperature, compared to Ag-ZSM-5 . The silver species are concluded to be of major importance for the catalytic activity at low temperature, while a high specific surface area and a high surface acidity are somewhat less important. The influence of the silver loading for methanol-SCR was studied in flow-reactor experiments and show that $\text{Ag}/\text{Al}_2\text{O}_3$ with 3 wt% Ag (sol-gel) gives NO_x reduction in a broad temperature interval, with high activity at low temperatures typical for exhaust gases from diesel and other lean burn engines. In order to investigate exclusively the influence of the types of silver species, catalysts with the same silver loading but different composition of silver species were prepared by different methods. The differences in the composition of silver species were investigated by TEM, UV-vis spectroscopy and H_2 -TPR. Fairly small silver species are suggested to be reduced during H_2 -TPR, possibly small silver clusters. The silver species reduced during the H_2 -TPR cannot be directly associated with the NO_x reduction to N_2 , likely owing to involvement of additional types of silver species in the methanol-SCR reactions. Comparisons of flow-reactor results with the characterization show that the temperature for NO_x reduction over $\text{Ag}/\text{Al}_2\text{O}_3$ during methanol-SCR conditions is determined by several types of small ($n < 7$) silver clusters, and/or small silver nanoparticles ($< \text{ca } 20 \text{ nm}$). Furthermore, silver nanoparticles are concluded to catalyse formation of N_2O , while the role of small silver species (ions and small clusters) is suggested to be promotion of N_2 formation.

Further experiments show that a moderate increase of the C/N molar ratio can enhance the lean NO_x reduction with methanol over $\text{Ag}/\text{Al}_2\text{O}_3$. In addition, the influence of O_2 and NO on the conversion of methanol over $\text{Ag}/\text{Al}_2\text{O}_3$ was investigated and found to be influenced by the supported silver species. Addition of H_2 to the methanol-SCR feed results in a small enhancement of N_2 formation at low temperature, but also in a higher formation of N_2O . Thus, addition of H_2 does not provide obvious benefits, but on the other hand formation of H_2 from methanol is observed. Surface species were studied in DRIFTS experiments and the hydrogen abstracted during the conversion of methanol is suggested to explain the high NO_x reduction at low temperature associated with oxygenated reducing agents, rather than the subsequently formed gaseous H_2 . This can explain why a high low-temperature activity during methanol-SCR conditions is seen also when not so much H_2 is present in the outlet

of the reactor, but more H₂O. The effect of the formed hydrogen is likely similar to the effect of H₂ added to HC-SCR applications, where several suggestions for its origin have been made. In the present work reduction of silver was revealed by UV-vis spectroscopy after exposure of Ag/Al₂O₃ to H₂ and a methanol-SCR gas mixture, respectively. Moreover, NO-TPD after adsorption of NO in oxygen excess with/without H₂, demonstrates the influence of H₂ on the desorption of NO_x.

To conclude, the results show that the low-temperature activity for lean NO_x reduction with methanol over Ag/Al₂O₃ is highly dependent on the composition of supported silver species and their interplay with adsorbed and gas phase species. This work provides new insights in the importance of small silver species for the selectivity to N₂ and the importance of somewhat larger silver species for catalytic activity at low temperature. The observed formation of H₂ from methanol gives an indication of that the high low-temperature activity associated with oxygenated reducing agents may be connected to the release of hydrogen atoms during the conversion of the oxygenate. An effect of hydrogen observed in the present work is reduction of silver after exposure to H₂ and a methanol-SCR gas mixture, respectively.

7. Outlook

In order to get a better understanding of the role of supported silver species for the lean NO_x reduction with methanol, further characterization is desirable. Useful techniques are TEM with high resolution, XPS after more extensive reduction than what was used in Paper III, X-ray absorption spectroscopy (XAS) in order to study oxidation and reduction processes of silver species and X-ray diffraction (XRD) for studies of crystallinity and possibly silver particle size. In addition in-situ techniques could provide information regarding the silver species during reaction conditions, for example in-situ UV-vis spectroscopy.

The methanol-SCR reaction mechanisms are not yet fully understood, even if suggestions have been made in the literature. Further insights could be gained from carefully tailored DRIFTS experiments, preferably using an instrument with fast response. Also modelling or density functional theory (DFT) calculations could provide further confirmation of suggested reaction mechanisms or information of the stability of silver species or other surface species during reaction conditions.

The NO_x reduction achieved during methanol-SCR over $\text{Ag}/\text{Al}_2\text{O}_3$ in the present work is not high enough for the system to be a commercially viable alternative. However, the current findings are likely applicable also for other oxygenated reducing agents. For example ethanol has shown high NO_x reduction over $\text{Ag}/\text{Al}_2\text{O}_3$. It would, thus, be interesting to evaluate other oxygenates as reducing agents and investigate how the choice of reducing agent influences the formation of hydrogen, the reduction of silver and the formation of adsorbed and gas phase species. In addition the influence of other gas phase species should be investigated, like water and CO_2 .

Acknowledgements

This work has been funded by the Swedish Energy Agency and performed within the Competence Centre for Catalysis, which is hosted by Chalmers University of Technology and financially supported by the Swedish Energy Agency and the member companies: AB Volvo, ECAPS AB, Haldor Topsøe A/S, Scania CV AB, Volvo Car Corporation AB and Wärtsilä Finland Oy. Financial support from Knut and Alice Wallenberg Foundation, Dnr KAW 2005.0055, is acknowledged.

I would also like to thank:

Associate Professor **Hanna Härelind**, my main supervisor, for all inspiring and fun discussions and for always having time for me. I have had a great time working with you!

Professor **Magnus Skoglundh**, my co-supervisor and examiner, for great support and thorough reading of all my manuscripts. Thanks for all help during my PhD period.

Xueting, my master thesis worker who became a PhD student and my friend, for great collaboration and thorough work contributing to Papers V and VI.

Stefanie, my friend and former office mate, for great support and inspiring discussions.

Ann Jakobsson, for help with administrative issues.

All badminton playing colleagues, **Xueting, Stefanie, Sheedeh, Kirsten, Kurnia, Anna, Chris, Anastasia, Maria, Oana, Natalia**. It has been a lot of fun playing with you!

All former and present **friends** and **colleagues** at KCK and TYK for nice discussions and creating a good working atmosphere.

My **family** for all support and distraction from work.

References

1. Granger P, Parvulescu VI (2011) Chem Rev 111 (5):3155-3207.
2. Twigg MV (2011) Catal Today 163 (1):33-41.
3. Burch R (2004) Catal Rev-Sci Eng 46 (3-4):271-333.
4. Heck RM, Farrauto RJ (2001) Appl Catal, A 221 (1-2):443-457.
5. Skalska K, Miller JS, Ledakowicz S (2010) Sci Total Environ 408 (19):3976-3989.
6. European Commission Biofuels in the European Union - A Vision for 2030 and beyond, Final report of the Biofuels Research Advisory Council, http://ec.europa.eu/research/energy/pdf/biofuels_vision_2030_en.pdf Accessed 2015-03-18.
7. Olah GA, Goepfert A, Prakash GKS (2009), *Beyond oil and gas : the methanol economy*, 2nd edn, Wiley-VCH, Weinheim
8. Eurostat Emissions of nitrogen oxides (NO_x) by source sector, <http://ec.europa.eu/eurostat/> Accessed 2015-03-18.
9. Tham YF, Chen JY, Dibble RW (2009) Proc Combust Inst 32:2827-2833.
10. Johnson TV (2009) Int J Engine Res 10 (5):275-285.
11. Roy S, Hegde MS, Madras G (2009) Appl Energy 86 (11):2283-2297.
12. Klingstedt F, Arve K, Eranen K, Murzin DY (2006) Accounts Chem Res 39 (4):273-282.
13. DieselNet Emission Standards, <http://dieselnet.com/> Accessed 2015-04-08.
14. Zheng M, Reader GT (2004) Energy Conv Manag 45 (15-16):2473-2493.
15. Burch R, Breen JP, Meunier FC (2002) Appl Catal B 39 (4):283-303.
16. Nakatsuji T, Yasukawa R, Tabata K, Ueda K, Niwa M (1998) Appl Catal B 17 (4):333-345.
17. He H, Zhang XL, Wu Q, Zhang CB, Yu YB (2008) Catal Surv Asia 12 (1):38-55.
18. Fritz A, Pitchon V (1997) Appl Catal B 13 (1):1-25.
19. Heck RM, Farrauto RJ (1995), *Catalytic Air Pollution Control, Commercial Technology*, Van Nostrand Reinhold, New York
20. Meunier FC, Breen JP, Zuzaniuk V, Olsson M, Ross JRH (1999) J Catal 187 (2):493-505.
21. Miyadera T (1998) Appl Catal B 16 (2):155-164.
22. Tabata M, Tsuchida H, Miyamoto K, Yoshinari T, Yamazaki H, Hamada H, Kintaichi Y, Sasaki M, Ito T (1995) Appl Catal B 6 (2):169-183.
23. Seker E, Cavataio J, Gulari E, Lorpongpaiboon P, Osuwan S (1999) Appl Catal, A 183 (1):121-134.

24. Kannisto H, Karatzas X, Edvardsson J, Pettersson LJ, Ingelsten HH (2011) *Appl Catal B* 104 (1-2):74-83.
25. Iwamoto M, Yahiro H, Yuu Y, Shundo S, Mizuno N (1990) *Shokubai* 32:430-433.
26. Held W, König A, Richter T, Puppe L (1990) SAE paper 900496.
27. Liu ZM, Woo SI (2006) *Catal Rev-Sci Eng* 48 (1):43-89.
28. Chorkendorff I, Niemantsverdriet JW (2003), *Concepts of Modern Catalysis and Kinetics*, Wiley-VCH GmbH & Co. KGaA, Weinheim
29. Burrows A, Holman J, Parsons A, Pilling G, Price G (2009), *Chemistry3, introducing inorganic, organic and physical chemistry*, Oxford University Press Inc., New York
30. Miyadera T (1993) *Appl Catal B* 2 (2-3):199-205.
31. Masuda K, Tsujimura K, Shinoda K, Kato T (1996) *Appl Catal B* 8 (1):33-40.
32. Ukisu Y, Miyadera T, Abe A, Yoshida K (1996) *Catal Lett* 39 (3-4):265-267.
33. Bethke KA, Kung HH (1997) *J Catal* 172 (1):93-102.
34. Hoost TE, Kudla RJ, Collins KM, Chattha MS (1997) *Appl Catal B* 13 (1):59-67.
35. Arve K, Capek L, Klingstedt F, Eranen K, Lindfors LE, Murzin DY, Dedecek J, Sobalik Z, Wichterlova B (2004) *Top Catal* 30-1 (1-4):91-95.
36. Meunier FC, Ukropec R, Stapleton C, Ross JRH (2001) *Appl Catal B* 30 (1-2):163-172.
37. Aoyama N, Yoshida K, Abe A, Miyadera T (1997) *Catal Lett* 43 (3-4):249-253.
38. Wang ZM, Yamaguchi M, Goto I, Kumagai M (2000) *Phys Chem Chem Phys* 2 (13):3007-3015.
39. Takagi K, Kobayashi T, Ohkita H, Mizushima T, Kakuta N, Abe A, Yoshida K (1998) *Catal Today* 45 (1-4):123-127.
40. Luo YM, Hao JM, Hou ZY, Fu LX, Li RT, Ning P, Zheng XM (2004) *Catal Today* 93-5:797-803.
41. Kannisto H, Ingelsten HH, Skoglundh M (2009) *J Mol Catal A: Chem* 302 (1-2):86-96.
42. She X, Flytzani-Stephanopoulos M (2006) *J Catal* 237 (1):79-93.
43. Sazama P, Capek L, Drobna H, Sobalik Z, Dedecek J, Arve K, Wichterlova B (2005) *J Catal* 232 (2):302-317.
44. Konova P, Arve K, Klingstedt F, Nikolov P, Naydenov A, Kumar N, Murzin DY (2007) *Appl Catal B* 70 (1-4):138-145.
45. Tamm S, Ingelsten HH, Palmqvist AEC (2008) *J Catal* 255 (2):304-312.
46. Parvulescu VI, Cojocaru B, Parvulescu V, Richards R, Li Z, Cadigan C, Granger P, Miquel P, Hardacre C (2010) *J Catal* 272 (1):92-100.
47. Musi A, Massiani P, Brouri D, Trichard JM, Da Costa P (2009) *Catal Lett* 128 (1-2):25-30.
48. Wu Q, He H, Yu YB (2005) *Appl Catal B* 61 (1-2):107-113.

49. Lindfors LE, Eranen K, Klingstedt F, Murzin DY (2004) *Top Catal* 28 (1-4):185-189.
50. Yoon DY, Park JH, Kang HC, Kim PS, Nam IS, Yeo GK, Kil JK, Cha MS (2011) *Appl Catal B* 101 (3-4):275-282.
51. Bogdanchikova N, Meunier FC, Avalos-Borja M, Breen JP, Pestryakov A (2002) *Appl Catal B* 36 (4):287-297.
52. Iliopoulou EF, Evdou AP, Lemonidou AA, Vasalos IA (2004) *Appl Catal, A* 274 (1-2):179-189.
53. Kim MK, Kim PS, Baik JH, Nam IS, Cho BK, Oh SH (2011) *Appl Catal B* 105 (1-2):1-14.
54. Kiattisirikul N, Chaisuk C, Praserttham P (2004) *Catal Today* 97 (2-3):129-135.
55. Sadokhina NA, Prokhorova AF, Kvon RI, Mashkovskii IS, Bragina GO, Baeva GN, Bukhtiyarov VI, Stakheev AY (2012) *Kinet Catal* 53 (1):107-116.
56. da Silva R, Cataluna R, Martinez-Arias A (2009) *Catal Today* 143 (3-4):242-246.
57. Martinez-Arias A, Fernandez-Garcia M, Iglesias-Juez A, Anderson JA, Conesa JC, Soria J (2000) *Appl Catal B* 28 (1):29-41.
58. Shimizu K, Shibata J, Yoshida H, Satsuma A, Hattori T (2001) *Appl Catal B* 30 (1-2):151-162.
59. Richter M, Bentrup U, Eckelt R, Schneider M, Pohl MM, Fricke R (2004) *Appl Catal B* 51 (4):261-274.
60. Keshavaraja A, She X, Flytzani-Stephanopoulos M (2000) *Appl Catal B* 27 (1):L1-L9.
61. Son IH, Kim MC, Koh HL, Kim KL (2001) *Catal Lett* 75 (3-4):191-197.
62. Guo Y, Chen J, Kameyama H (2011) *Appl Catal, A* 397 (1-2):163-170.
63. Kameoka S, Ukisu Y, Miyadera T (2000) *Phys Chem Chem Phys* 2 (3):367-372.
64. Li ZJ, Flytzani-Stephanopoulos M (1997) *Appl Catal, A* 165 (1-2):15-34.
65. Seijger GBF, Niekerk PV, Krishna K, Calis HPA, van Bekkum H, van den Bleek CM (2003) *Appl Catal B* 40 (1):31-42.
66. Sato S, Yoshihiro Y, Yahiro H, Mizuno N, Iwamoto M (1991) *Applied Catalysis* 70 (1):L1-L5.
67. Shi C, Cheng MJ, Qu ZP, Yang XF, Bao XH (2002) *Appl Catal B* 36 (3):173-182.
68. Bartolomeu R, Henriques C, da Costa P, Ribeiro F (2011) *Catal Today* 176 (1):81-87.
69. Shi C, Cheng MJ, Qu ZP, Bao XH (2005) *J Mol Catal A: Chem* 235 (1-2):35-43.
70. Shibata J, Shimizu K, Takada Y, Shichia A, Yoshida H, Satokawa S, Satsuma A, Hattori T (2004) *J Catal* 227 (2):367-374.
71. Shibata J, Takada Y, Shichi A, Satokawa S, Satsuma A, Hattori T (2004) *J Catal* 222 (2):368-376.
72. Satokawa S (2000) *Chem Lett* 29 (3):294-295.

73. Satokawa S, Shibata J, Shimizu K, Atsushi S, Hattori T (2003) *Appl Catal B* 42 (2):179-186.
74. Arve K, Backman H, Klingstedt F, Eranen K, Murzin DY (2007) *Appl Catal B* 70 (1-4):65-72.
75. Zhang XL, He H, Ma ZC (2007) *Catal Commun* 8 (2):187-192.
76. Johnson WL, Fisher GB, Toops TJ (2012) *Catal Today* 184 (1):166-177.
77. Breen JP, Burch R (2006) *Top Catal* 39 (1-2):53-58.
78. Shimizu K, Tsuzuki M, Kato K, Yokota S, Okumura K, Satsuma A (2007) *J Phys Chem C* 111 (2):950-959.
79. Brosius R, Arve K, Groothaert MH, Martens JA (2005) *J Catal* 231 (2):344-353.
80. Kannisto H, Ingelsten HH, Skoglundh M (2009) *Top Catal* 52 (13-20):1817-1820.
81. Korhonen ST, Beale AM, Newton MA, Weckhuysen BM (2011) *J Phys Chem C* 115 (4):885-896.
82. Burch R, Breen JP, Hill CJ, Krutzsch B, Konrad B, Jobson E, Cider L, Eranen K, Klingstedt F, Lindfors LE (2004) *Top Catal* 30-1 (1-4):19-25.
83. Shibata J, Shimizu K, Satokawa S, Satsuma A, Hattori T (2003) *Phys Chem Chem Phys* 5 (10):2154-2160.
84. Wichterlova B, Sazama P, Breen JP, Burch R, Hill CJ, Capek L, Sobalik Z (2005) *J Catal* 235 (1):195-200.
85. Chansai S, Burch R, Hardacre C, Breen J, Meunier F (2010) *J Catal* 276 (1):49-55.
86. Shimizu K, Sawabe K, Satsuma A (2011) *Catal Sci Technol* 1 (3):331-341.
87. Sayin C, Ilhan M, Canakci M, Gumus M (2009) *Renewable Energy* 34:1261–1269.
88. Methanol_Institute China: The Leader in Methanol Transportation, <http://www.methanol.org/Methanol-Basics/Resources/China-Methanol.aspx> Accessed 2012-06-07.
89. SPIRETH, <http://www.spireth.com/> Accessed 2015-03-20.
90. Marine Methanol, <http://www.marinemethanol.com/> Accessed 2015-03-20.
91. Brusstar M, Stuhldreher M, Swain D, Pidgeon W (2002) SAE paper 2002-01-2743.
92. Seko T, Kuroda E, Hamano Y (1998) SAE paper 980531.
93. Udayakumar R, Sundaram S, Sivakumar K (2004) SAE paper 2004-01-0096.
94. Huang ZH, Lu HB, Jiang DM, Zeng K, Liu B, Zhang JQ, Wang XB (2004) *Proceedings of the Institution of Mechanical Engineers Part D-Journal of Automobile Engineering* 218 (D9):1011-1024.
95. Song RZ, Liu J, Wang LJ, Liu SH (2008) *Energy Fuels* 22 (6):3883-3888.
96. Zhu TL, Hao RM, Fu LX, Li JH, Liu ZM (2005) *React Kinet, Mech Catal* 84 (1):61-67.
97. Tamm S, Ingelsten HH, Skoglundh M, Palmqvist AEC (2009) *Top Catal* 52 (13-20):1813-1816.

98. Tamm S, Ingelsten HH, Skoglundh M, Palmqvist AEC (2010) *J Catal* 276 (2):402-411.
99. Ertl G (1999), *Preparation of solid catalysts*, Wiley-VCH, Weinheim
100. Bowker M (1998), *The Basis and Applications of Heterogenous Catalysis*, Oxford University Press, Oxford
101. Sun PP, Song HI, Kim TY, Min BJ, Cho SY (2014) *Industrial & Engineering Chemistry Research* 53 (52):20241-20246.
102. Holmberg K (2004) *J Colloid Interface Sci* 274 (2):355-364.
103. Pileni MP (2003) *Nat Mater* 2 (3):145-150.
104. Haber J, Machej T, Czeppe T (1985) *Surface Science* 151 (1):301-310.
105. Baláž P (2008), *Mechanochemistry in nanoscience and minerals engineering*, Springer, Berlin; London
106. Brunauer S, Emmett PH, Teller E (1938) *J Am Chem Soc* 60:309-319.
107. Chorkendorff I, Niemantsverdriet JW (2003) *Surface area*. In: *Concepts of modern catalysis and kinetics*. Wiley-VCH GmbH & Co. KGaA, pp 185-190
108. Niemantsverdriet JW (2000), *Spectroscopy in Catalysis*, Second, Completely Revised Edition edn, Wiley-VCH Verlag GmbH, Weinheim
109. Chatwal GR, Anand SK, Arora M, Anand A, ebrary (2009), *Spectroscopy: atomic and molecular*, Himalaya Pub. House, Mumbai
110. Kaur H (2009), *Spectroscopy*, Pragati Prakashan, Meerut, IND
111. Wagner JM (2011), *X-ray photoelectron spectroscopy*, Nova Science Publishers, New York
112. van der Heide P (2011), *X-Ray Photoelectron Spectroscopy : An Introduction to Principles and Practices*, John Wiley & Sons, Hoboken, NJ, USA
113. Lok BM, Marcus BK, Angell CL (1986) *Zeolites* 6 (3):185-194.
114. Höhne GWH, Hemminger WF, Flammersheim HJ, SpringerLink A, SpringerLink (2003), *Differential Scanning Calorimetry*, Springer, Berlin, Heidelberg. doi:10.1007/978-3-662-06710-9.
115. Wang-Hansen C, Kamp CJ, Skoglundh M, Andersson B, Carlsson P-A (2011) *J Phys Chem C* 115 (32):16098-16108.
116. Gross JH, SpringerLink (2010), *Mass spectrometry: a textbook*, Springer, Berlin; London
117. Masters SG, Chadwick D (1999) *Appl Catal B* 23 (4):235-246.
118. Tamm S, Ingelsten HH, Palmqvist AEC (2008) *Catal Lett* 123 (3-4):233-238.
119. Bion N, Saussey J, Haneda M, Daturi M (2003) *J Catal* 217 (1):47-58.
120. Thibault-Starzyk F, Seguin E, Thomas S, Daturi M, Arnolds H, King DA (2009) *Science* 324 (5930):1048-1051.

121. Kannisto H, Arve K, Pingel T, Hellman A, Harelind H, Eranen K, Olsson E, Skoglundh M, Murzin DY (2013) *Catal Sci Technol* 3 (3):644-653.
122. Gang L, Anderson BG, van Grondelle J, van Santen RA (2003) *Appl Catal B* 40 (2):101-110.
123. Sayah E, Brouri D, Massiani P (2013) *Catal Today* 218:10-17.
124. Tamm S, Vallim N, Skoglundh M, Olsson L (2013) *J Catal* 307:153-161.
125. Azis MM, Harelind H, Creaser D (2015) *Catal Sci Technol* 5 (1):296-309.
126. Sadokhina NA, Doronkin DE, Pributkov PV, Bukhtiyarov VI, Kvon RI, Stakheev AY (2011) *Top Catal* 54 (16-18):1190-1196.
127. Tamm S (2013) *Catal Lett* 143 (9):957-965.
128. Chaieb T, Delannoy L, Louis C, Thomas C (2013) *Appl Catal B* 142:780-784.
129. Thomas C (2015) *Appl Catal B* 162:454-462.
130. Tamm S, Ingelsten HH, Skoglundh M, Palmqvist AEC (2009) *Appl Catal B* 91 (1-2):234-241.
131. Stegelmann C, Stoltze P (2004) *J Catal* 226 (1):129-137.
132. Busca G (1996) *Catal Today* 27 (3-4):457-496.
133. Matyshak VA, Berezina LA, Sil'Chenkova ON, Tret'Yakov VF, Lin GI, Rozovskii AY (2009) *Kinet Catal* 50 (1):111-121.